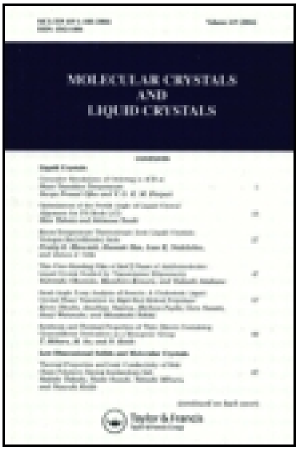

Molecular Crystals and Liquid Crystals Science and Technology. Section A. Molecular Crystals and Liquid Crystals
Publication details, including instructions for authors and subscription information:
http://www.tandfonline.com/loi/gmcl19

Second Sound and Nonlinear Optical Phenomena in Smectic A Liquid Crystals

G. F. Kventsel [a] & B. I. Lembrikov [a]
[a] Department of Chemistry, Technion-Israel Institute of Technology, Haifa, 32000, Israel
Version of record first published: 24 Sep 2006.

Mol. Cryst. Liq. Cryst., 1996, Vol. 282, pp. 145–189
Reprints available directly from the publisher
Photocopying permitted by license only

SECOND SOUND AND NONLINEAR OPTICAL PHENOMENA IN SMECTIC A LIQUID CRYSTALS

G. F. KVENTSEL and B. I. LEMBRIKOV
Department of Chemistry, Technion – Israel Institute of Technology,
Haifa, 32000, Israel

Abstract. We investigated theoretically the nonlinear phenomena (a self-focusing, a self-trapping, stimulated light scattering and four-wave mixing) in smectic A liquid crystals (SA) caused by a new physical mechanism of cubic nonlinearity determined by the propagating mode of a layer normal displacement, or the so-called second sound. A nonlinear part of a refractive index caused by a layer normal deformation which is responsible for a self-focusing effect, and a gain coefficient in the case of a stimulated light scattering (SLS) on the second sound are one or two orders of magnitude greater than the similar quantities for isotropic organic liquids. The light-induced dynamic grating of layer deformations generates a high-frequency longitudinal electric field due to the flexoelectric effect. The light-induced dynamic grating of layer normal displacement ultimately excites a rotational hydrodynamic flow with a considerable velocity. Using the slow varying amplitude approximation we calculated the light wave and second sound wave amplitudes explicitly for some important cases.

1. INTRODUCTION

Liquid crystals are highly nonlinear materials due to their unique complex physical structures, and their physical properties (temperature, molecular orientation, mass density, etc.) are easily perturbed by an applied optical field.[1] The nonlinear optics of liquid crystals emerged as a separate field of liquid crystals study, and the nonlinear optical phenomena in liquid crystals have been thoroughly investigated both theoretically and experimentally.[1–5] The state-of-the-art is reviewed in Ref. [1].

In general, the nonlinear optical phenomena may be described in terms of optically induced refractive index changes.[1] The major mechanisms responsible for the refractive index changes in liquid crystals are the optically induced changes in the molecular reorientation angle $\Delta\theta$, in the temperature ΔT and in the mass density $\Delta\rho$.[1–5] The more complicated nonlinear effects such as orientational-temperature and flow-orientational coupling are also possible.[1] Nematic liquid crystals (NLC) so far remain the main focus of nonlinear optical investigations and applications due to their giant orientational and thermal nonlinearity and their sensitivity to comparatively low light intensity. However, NLC have at least two disadvantages from the point of view of nonlinear optical applications. Firstly, despite the extraordinarily large orientational nonlinearity, the slow decay time of the reorientation remains as a major limitation in practical device applications.[5] Secondly, the large light scattering loss limits the possibility of optical processes in NLC requiring longer interaction length than a few hundred microns - the typical extinction length in NLC.[1] These limitations are essential for the novel applications of liquid crystals in high peak-power lasers, where the elements are required to be large, low in loss (both in terms of scattering and absorption), resistant to laser damage of multijouls cm^{-2} fluence levels and to possess a fast response.[6] The basic physics of laser induced molecular reorientation, thermal, density and flow phenomena in the smectic phase are qualitatively similar to those occuring in the nematic phase.[1] However, smectic liquid crystals (SA) are highly viscous, and they do not flow as easily as nematics do.[1,7,8] The smectics tendency to have layered structures imposes a further restriction on the reorientation by an external field.[1] The order parameter's dependence on the temperature is less drastic than in the nematic phase, and thus the refractive indices $n_{||}$ and $n_{\perp}$ are not sensitively dependent on the temperature.[1] Consequently, the optical nonlinearity of SA caused by the orientational and thermal mechanisms is comparatively small. The Brillouin and electronic cubic nonlinearities in SA while being fast enough have approximately the same order of magnitude as the ones in organic liquids do since their elastic constants associated with the bulk compression and their molecular susceptibilities are approximately of the same order of magnitude.[1,7–11]

In a number of works[12–18] we investigated theoretically the self-focusing, self-trapping, stimulated light scattering (SLS) and four-wave mixing (FWM)[19] in SA caused by the new mechanism of the cubic nonlinearity which is determined by the propagating mode of a layer normal displacement, or the so-called second sound.[7,8] The temporal, spatial and energetic characteristics of the new nonlinearity mechanism are evaluated. It turned out that this mechanism combines the typical features of the orientational nonlinearity and the electrostrictive one, since it occurs without a change of a mass density, strongly depends on the light polarization and propagation direction, and, on the other hand, has a frequency dependence of a resonance form, short response time and the characteristic energy which is intermediate between the orientational energy and bulk compression's one.

The nonlinear optical processes are essentially different when the layer normal deformation exists and when it is absent. In the second case SA behaves similarly to NLC as a two-dimensional liquid in a plane of a layer.[14]

The ordinary and extraordinary beams undergo a self-focusing and a self-trapping in a form of a transverse spatial soliton due to the layer normal deformation. A nonlinear part of the refraction index determined by this deformation is about 10^{-10} *esu* which is one or two orders of magnitude greater than the one for the orientational Kerr effect and electrostriction in organic liquids. The self-focusing and self-trapping of the extraordinary beam strongly depends on its propagation direction and polarization, and these effects are possible only when the angle between the beam vector and the wave vector is sufficiently small. The propagation of a bright surface-guided wave is possible at an interface between a linear medium and SA.[18] In the absence of the layer normal deformation the arbitrary polarized light propagating in a layer plane undergoes a self-phase modulation.

The stimulated scattering of two arbitrary polarized light waves on the layer deformations transforms into a partly degenerate FWM[16] because each wave splits into an ordinary wave and an extraordinary one due to the optical anisotropy of SA.[20] Their interference creates the dynamic grating of the layer displacement. The light waves coupling is strong when their frequency difference is close to the second sound frequency. Two light waves with the lower frequency are amplified while two waves with the greater frequency are depleted. The gain coefficient is one or two orders of magnitude greater than the one in the case of the ordinary Brillouin scattering in isotropic organic liquids. The combination of the optical anisotropy and nonlinearity gives rise to the additional components of the fundamental light waves. The spectrum of scattered waves consists of 20 harmonics with the Stokes, anti-Stokes and fundamental frequencies and combination wave vectors unlike the ordinary Brillouin scattering when one Stokes wave and one anti-Stokes wave exist.[16]

The two-wave mixing corresponds to the particular case of SLS when each incident light wave is polarized in the incidence plane, or normal to it.[12,14–16]

The nondegenerate FWM on a second sound is to some extent analogous to the Brillouin enhanced FWM (BEFWM)[21–24] which combines the possibility of the parametric amplification and phase conjugation. Four interfering light waves with the frequency differences close to the second sound frequency generate a dynamic grating of the layer displacement which consists of 6 harmonics with the essentially different frequencies and wave vectors. The energy and momentum conservation laws for the frequencies and wave vectors of the fundamental light waves scattering on this grating are met automatically which permits the effective energy transfer from the pumping wave with the largest frequency to the signal wave with the lowest frequency. Two waves with the intermediate frequencies form the spatially localized soliton-like structures. If the two pairs of waves counterpropagate, then the phase conjugation and amplification of the phase-conjugate wave occur. The additional components of the fundamental light waves are created analogously to SLS. The spectrum of the scattered harmonics this time consists of 24 nondegenerate harmonics with the combination frequencies and wave vectors due to the nondegenerate character of the process.[17]

Unlike NLC, where the purely orientational excitations are possible without the hydrodynamic flow of a material as a whole, in SA the light-induced layer displacement varying with time inevitably excites the hydrodynamic motion. A hydrodynamic velocity depending on the light intensity may reach a value of 10 cm sec^{-1}.[17] The flow represents a complicated pattern[25] which is periodic in space and oscillatory in time. In the conducting SA an alternating component of an electric current determined by the hydrodynamic velocity is much larger than a direct current determined by low-mobility ions. The light-induced dynamic grating generates a longitudinal high-frequency electric field due to the flexoelectric effect. The light-induced electric field can reach a value comparable with the one in NLC. The longitudinal electric field behaves as a surface wave at the boundary between SA and a linear medium.[15-17] This field also breaks the inversion symmetry of SA and permits a second harmonic generation (SHG) for each incident wave. The theoretical results for SLS and FWM show a good accord with the experimental data obtained by I. C. Khoo and co-workers.[9]

2. THE BASIC EQUATIONS

The quantitative description of a nonlinear optical effect usually starts with a set of coupled wave equations with the nonlinear susceptibilities acting as the coupling coefficients.[19] This coupled-wave approach can also be generalized to include waves other than electromagnetic, such as acoustic wave, shear waves etc.[19] We are starting with the equation of motion of a layer normal displacement in an external electric field. The hydrodynamics of SA has been analyzed in Ref. [7], [8], [26]-[30]. The effects connected with the first and second sound, respectively, can be considered separately since the elastic constant associated with the bulk compression is much larger than the elastic constant B associated with the layer compression.[7,8] We are interested in the phenomena connected with the second sound. In such a case SA is assumed to be incompressible, and the system of equations describing the hydrodynamics of SA far from the phase transition when the temperature is assumed to be constant takes the form[7,8]:

$$\begin{aligned}
\mathrm{div}\vec{v} &= 0 &(1)\\
\rho\frac{\partial v_i}{\partial t} &= -\frac{\partial \Pi}{\partial x_i}+\Lambda_i+\frac{\partial \sigma'_{ik}}{\partial x_k} &(2)\\
\vec{\Lambda} &= -\frac{\delta F}{\delta \vec{u}} &(3)\\
\sigma'_{ik} &= \alpha_0\delta_{ik}\mathcal{A}_{ll}+\alpha_1\delta_{iz}\mathcal{A}_{zz}+\alpha_4\mathcal{A}_{ik}+\alpha_{56}\left(\delta_{iz}\mathcal{A}_{zk}+\delta_{kz}\mathcal{A}_{zi}\right)+\\
&\quad \alpha_7\delta_{iz}\delta_{kz}\mathcal{A}_{ll} &(4)\\
\mathcal{A}_{ik} &= \frac{1}{2}\left(\frac{\partial v_i}{\partial x_k}+\frac{\partial v_k}{\partial x_i}\right) &(5)\\
v_z &= \frac{\partial u}{\partial t} &(6)
\end{aligned}$$

where v_i is the hydrodynamic velocity, ρ is a mass density, Π is a pressure, $\vec{\Lambda}$ is the generalized force density, σ'_{ik} is the viscous stress tensor, α_{ik} are the viscosity Leslie coefficients, F is the free energy density of an incompressible SA. In the presence of an external electric field $\vec{E}$ it takes the form[7,20]:

$$F=\frac{1}{2}B\left(\frac{\partial u}{\partial z}\right)^2+\frac{1}{2}\mathcal{K}\left(\frac{\partial^2 u}{\partial x^2}+\frac{\partial^2 u}{\partial y^2}\right)^2-\frac{1}{8\pi}\varepsilon_{ik}E_iE_k \quad (7)$$

where $\mathcal{K}$ is the Frank elastic constant associated with the orientational energy, and ε_{ik} is the dielectric constant tensor containing the terms linear on the layer deformations. It has the form[7,8,26,27]:

$$\begin{aligned}
\varepsilon_{xx} &= \varepsilon_{yy}=\varepsilon_\perp+a_\perp\frac{\partial u}{\partial z}\\
\varepsilon_{zz} &= \varepsilon_{||}+a_{||}\frac{\partial u}{\partial z}\\
\varepsilon_{xz} &= \varepsilon_{zx}=-\varepsilon_a\frac{\partial u}{\partial x}\\
\varepsilon_{yz} &= \varepsilon_{zy}=-\varepsilon_a\frac{\partial u}{\partial y}\\
\varepsilon_a &= \varepsilon_{||}-\varepsilon_\perp &(8)
\end{aligned}$$

where $\varepsilon_{||}$ and $\varepsilon_\perp$ are the diagonal values of ε_{ik} along the optical axis and normal to it, respectively, and $a_{||}, a_\perp$ are the phenomenological dimensionless coefficients of an order of magnitude of unity.[26] The X and Y axes are chosen to be in the plane of the layer, and the Z axis coinciding with the optical axis of SA is normal to the layer. In an incompressible SA the free energy density F does not depend on the bulk compression, and therefore

$$\Pi\equiv 0 \quad (9)$$

The condition of the layer continuity (6) is specific for SA. It is valid in the case of the second sound excitation when the slow process of permeation can be ignored.[7,8] The layer displacement $\vec{u}(\vec{r},t)$ has by definition only one component normal to the layer plane[7,8,26,27]:

$$\vec{u} = (0, 0, u) \tag{10}$$

Therefore

$$\vec{\Lambda} = (0, 0, \Lambda_z) \tag{11}$$

In the case of excitations depending on z the orientational terms in (7) can be neglected because for the typical values of B and $\mathcal{K} \sim 10^{-6}$ dyn[7,8]

$$\mathcal{K}k^2 \ll B \tag{12}$$

for any reasonable inverse spatial dimension k of the excitation considered. In general case when

$$\frac{\partial u}{\partial z} \neq 0$$

substituting the relationships (3)-(5), (7), (10) and (11) into the equation (2), taking into account the condition (1), applying to the equation (2) the operator rot rot, using the well-known identity[31]

$$\text{rot rot}\vec{v} = \text{grad div}\vec{v} - \nabla^2\vec{v}$$

and substituting the relationship (6) into the equation for v_z we obtain the equation of motion for the normal displacement $u(\vec{r},t)$ of a layer[12,15–17]:

$$-\rho\nabla^2\frac{\partial^2 u}{\partial t^2} + \left[\alpha_1\nabla_\perp^2\frac{\partial^2}{\partial z^2} + \frac{1}{2}(\alpha_4 + \alpha_{56})\nabla^2\nabla^2\right]\frac{\partial u}{\partial t} + B\nabla_\perp^2\frac{\partial^2 u}{\partial z^2} =$$
$$\frac{1}{8\pi}\nabla_\perp^2\{\frac{\partial}{\partial z}\left[a_\perp\left(E_x^2 + E_y^2\right) + a_\parallel E_z^2\right] - 2\varepsilon_a[\frac{\partial}{\partial x}(E_xE_z) +$$
$$+\frac{\partial}{\partial y}(E_yE_z)]\} \tag{13}$$

The equation (13) coincides with the equation of the second sound,[8] if an external electric field is absent and the viscosity terms are neglected. It is seen from (13) that the second sound can be excited by the arbitrary polarized light waves. However, the oblique direction of propagation of light waves with respect to a layer plane is necessary. We must use the values of E_i^2 which are time-averaged over the light frequency ω, since the second sound frequency Ω is of an order of magnitude of an ordinary sound frequency,[11,32–34] and therefore

$$\Omega \ll \omega \tag{14}$$

The homogeneous solution of the equation (13) represents the second sound wave with the dispersion relation[8]:

$$\Omega = s_0 k_s \sin\varphi \cos\varphi \tag{15}$$

where $s_0 = \sqrt{B/\rho}$ is the second sound velocity, $\vec{k}_s$ is the wave vector, and φ is the angle between $\vec{k}_s$ and its projection on the layer plane. The relaxation time of a homogeneous second sound wave has the form:

$$\tau_s = 2\rho \left[\alpha_1 \frac{(k_{sx}^2 + k_{sy}^2) k_{sz}^2}{k_s^2} + \frac{1}{2}(\alpha_4 + \alpha_{56}) k_s^2 \right]^{-1}$$

In the particular case when

$$\frac{\partial u}{\partial z} = 0 \tag{16}$$

we obtain from the relationships (1)-(11) the following equation instead of the equation (13)[14]:

$$\rho \frac{\partial^2 u}{\partial t^2} - \frac{1}{2}(\alpha_4 + \alpha_{56}) \nabla_\perp^2 \frac{\partial u}{\partial t} + \mathcal{K} \nabla_\perp^4 u = \frac{\varepsilon_a}{4\pi} \left[\frac{\partial}{\partial x}(E_x E_z) + \frac{\partial}{\partial y}(E_y E_z) \right] \tag{17}$$

In the absence of an external field $\vec{E}$ the equation (17) describes the overdamped undulation mode with the wave number k_u and the relaxation time τ_1[7,8]:

$$\tau_1 = \frac{(\alpha_4 + \alpha_{56})}{2\mathcal{K} k_u^2} \tag{18}$$

The inertial term in the left-hand side of (17) in such a case can be neglected.[7] However, in the case of two interfering light waves with the wave vectors $\vec{k}_{1,2}$ and the close frequencies $\omega_{1,2}$ such that

$$|\Delta\omega| = |\omega_1 - \omega_2| \ll \omega_1 \tag{19}$$

the first term in the left-hand side of (17) must be kept for sufficiently large

$$\left|\Delta\vec{k}\right| = \left|\vec{k}_1 - \vec{k}_2\right| \sim (10^3 \div 10^4)\ cm^{-1}$$

and

$$\Delta\omega > \frac{\alpha_i (\Delta k)^2}{\rho} \sim (10^6 \div 10^8)\ sec^{-1}$$

where the typical values of the material parameters were used: $\alpha_i \sim 1$ Poise, $\rho \sim 1$ g cm^{-3}.[7,8]

It is seen from the equation (17) that the undulation, or wave-like mode in SA is to some extent analogous to the overdamped orientational, or twist waves in NLC.[35-37] However, the twist waves in NLC exist without any hydrodynamic flow, while in SA the light-induced excitation of the undulation mode results in the hydrodynamic flow due to the condition (6). The equations (13) and (17) show that the orientational mechanism of the optical nonlinearity in SA represents the particular case of the new mechanism determined by the layer displacement as the main dynamic variable describing the medium. In general case both the normal and the tangential deformations of layers exist. The contribution of the normal deformations into the free energy is predominant. This case corresponds to the second sound.[7,8] In the particular case when the normal deformations of layers vanish the tangential deformations of layers remain which are connected with the small energy of the molecular reorientation inside a layer. This case corresponds to the purely dissipative undulation mode.[7,8] The equations of motion (13) and (17) permit a uniform description of a variety of nonlinear optical phenomena in SA.

The propagation and interaction of electromagnetic waves in a nonlinear medium is governed by the Maxwell equations which yield the wave equation[19]:

$$\text{rot rot}\vec{E} + \frac{1}{c^2}\frac{\partial^2 \vec{D}^L}{\partial t^2} = -\frac{1}{c^2}\frac{\partial^2 \vec{D}^{NL}}{\partial t^2} \tag{20}$$

where c is the light velocity in vacuum, and $\vec{D}^L$ and $\vec{D}^{NL}$ are the linear and nonlinear part of the electric induction, respectively, which have the form:

$$\vec{D}^L = \left(\varepsilon_\perp E_x, \varepsilon_\perp E_y, \varepsilon_\parallel E_z\right) \tag{21}$$

and

$$\begin{aligned} D_x^{NL} &= a_\perp \frac{\partial u}{\partial z} E_x - \varepsilon_a \frac{\partial u}{\partial x} E_z \\ D_y^{NL} &= a_\perp \frac{\partial u}{\partial z} E_y \\ D_z^{NL} &= a_\parallel \frac{\partial u}{\partial z} E_z - \varepsilon_a \frac{\partial u}{\partial x} E_x \end{aligned} \tag{22}$$

The electric field $\vec{E}$ and the total induction $\vec{D}$ also obey the condition[19,20]:

$$\text{div}\vec{D} = 0 \tag{23}$$

The amplitude A of an infinite plane wave is assumed to be dependent only on the coordinate in the Z direction normal to an interface between linear and nonlinear media[19]:

$$\vec{E} = \vec{e}\left\{A(z)\exp i(\vec{k}\vec{r} - \omega t) + \text{c.c.}\right\} \tag{24}$$

where $\vec{e}$ is the polarization unit vector. We use the slowly varying amplitude (SVA) approximation which is determined by the following condition[19]:

$$\left|\frac{\partial^2 A}{\partial z^2}\right| \ll \left|k\frac{\partial A}{\partial z}\right| \tag{25}$$

In the case of monochromatic light beam the field amplitude $A(\omega, \vec{r})$ depends not only on z but also on x and y,[19,20] and it is supposed that

$$\left|k\frac{\partial A}{\partial z}\right| \sim \left|\nabla_{\perp}^2 A\right| \tag{26}$$

where

$$\nabla_{\perp}^2 = \frac{\partial^2}{\partial x^2} + \frac{\partial^2}{\partial y^2} \tag{27}$$

is the transverse part of the Laplace operator. The condition (26) represents the so-called quasioptical approximation.[20] The SVA approximation makes it possible to obtain first order differential equations, or the so-called reduced equations for the complex amplitudes $A(z)$ defined as

$$A = |A(z)| \exp i\gamma(z) \tag{28}$$

where $\gamma(z)$ is a phase. The reduced equation for the amplitude $A(z)$ of an infinite plane wave has the form [19]:

$$-2ik_z\frac{\partial A}{\partial z}\left[1 - e_z\frac{(\vec{k}\vec{e})}{k_z}\right] = \frac{\omega^2}{c^2}(\vec{e}\vec{D}^{NL})\exp\left[-i\vec{k}\vec{r}\right] \tag{29}$$

For the light beams the reduced equation has the form[19]:

$$-2ik\frac{\partial A}{\partial z} - \nabla_{\perp}^2 A = \frac{\omega^2}{c^2}(\vec{e}\vec{D}^{NL})\exp(-i\vec{k}\vec{r}) \tag{30}$$

In the nonlinear optics the equation (30) can be used for the analysis of the self-focusing and self-defocusing effects.[19,20]

3. THE LIGHT SELF-ACTION EFFECTS IN SA

3.1 The Self-Focusing and Self-Trapping in SA

The passage of a laser beam through a nonlinear optical material is inevitably accompanied by intensity-dependent phase shift on the wave-front of the laser beam, as a result of the intensity-dependent refractive index and the finite beam size.[5] This phenomenon leads to the so-called self-action effects which result in a change in the form of an amplitude (self-focusing), in a change in a phase (self-phase modulation), in the state of polarization of the beam, and in the transforming of the beam into a stable filament with a constant width (self-trapping).[38]

In the case of the stationary self-focusing the light beam amplitudes $A_{o,e}$ are assumed to be time-independent.[19] This approach is valid when the pulse duration τ_p is much greater than the relaxation time typical for the nonlinearity mechanism.[38] In our case the relaxation time τ_s can be used with a characteristic perturbation dimension w instead of k_s^{-1}. In the case of SA due to its symmetry D_∞ [8] the XZ plane may be chosen in the plane of a light beam incidence, while the Y axis is normal to it. Using the equation of motion (13) we obtain for the time-independent perturbation:

$$B\frac{\partial^2 u}{\partial z^2} = \frac{1}{4\pi}\left\{\left[(a_{\|}e_{ez}^2 + a_{\perp}e_{ex}^2)\frac{\partial}{\partial z} - 2\varepsilon_a e_{ex}e_{ez}\frac{\partial}{\partial x}\right]|A_e|^2 + a_{\perp}\frac{\partial |A_o|^2}{\partial z}\right\} \quad (31)$$

where the transverse component E_y and the in-plane component $\vec{E}_e$ of the arbitrary polarized slab-shaped[39] light beam have the form, respectively:

$$E_y = A_o \exp i(\vec{k}_o\vec{r} - \omega t) + \text{c.c.} \quad (32)$$

$$\vec{E}_e = \vec{e}_e\left[A_e \exp i(\vec{k}_e\vec{r} - \omega t) + \text{c.c.}\right] \quad (33)$$

The simultaneous analysis of the equations (30) and (31) for the case of an arbitrary polarized light beam containing both components is very complicated because the amplitudes depend on the different coordinates. However, the beams can be assumed to propagate independently in the different directions due to the large optical anisotropy of SA: the ordinary beam propagates in the direction of its wave vector $\vec{k}_o$, while the extraordinary beam propagates along the beam vector $\vec{s} \perp \vec{e}_e$ which is determined by the angle θ_e [20]:

$$\theta_e = \arctan\left(\frac{\varepsilon_\perp}{\varepsilon_\|}\tan\theta_1\right) \quad (34)$$

where θ_1 is the angle between $\vec{k}_e$ and the Z axis. Therefore the layer deformations caused by each component are spatially separated. We consider two particular cases, when only one type of the polarization exists, and obtain the condition of validity of such an approach. It is useful to introduce the new coordinates (x', z') parallel and normal to the ordinary light beam propagation direction, respectively:

$$
\begin{aligned}
x' &= \frac{(\vec{k}_o\vec{r})}{k_o} = x\sin\theta_o + z\cos\theta_o \\
z' &= -x\cos\theta_o + z\sin\theta_o
\end{aligned}
\tag{35}
$$

where θ_o is the angle between $\vec{k}_o$ and the Z axis, and (x'', z'') which are parallel and normal to the beam vector $\vec{s}$, respectively:

$$
\begin{aligned}
x'' &= x\sin\theta_e + z\cos\theta_e \\
z'' &= -x\cos\theta_e + z\sin\theta_e
\end{aligned}
\tag{36}
$$

We are interested in the spatially localized solutions of the type:[39]

$$
\begin{aligned}
\lim_{z'\to\infty} |A_o(z')| &= 0 \\
\frac{\partial |A_o|}{\partial z'}|_{z'=0} &= 0 \\
|A_o(0)| &= |A_{omax}|
\end{aligned}
\tag{37}
$$

and the analogous solutions for $|A_e|$. Consider first the situation when only the ordinary beam propagates, and

$$|A_e| = 0 \tag{38}$$

In such a case the reduced equation for the amplitude A_o represents the well-known nonlinear Schrödinger equation (NSE)[40] with the positive definite coefficient of the term cubic on the amplitude A_o:

$$\frac{\omega^2}{c^2}\frac{a_\perp^2}{8\pi B k_o} > 0 \tag{39}$$

which corresponds to the stationary two-dimensional self-focusing of the light beam[20,40] with the nonlinear part n_{o2} of the refractive index:

$$n_{o2} = \frac{a_\perp^2}{8\pi B\sqrt{\varepsilon_\perp}} \tag{40}$$

Using the typical values $\sqrt{\varepsilon_\perp} = 1.5$, [5] $B \sim (10^7 \div 10^8)$ erg cm^{-3},[7,8,34] and $a_\perp \sim 1$, [26] we obtain $n_{o2} \sim (3\cdot 10^{-10} \div 3\cdot 10^{-9})$ esu which is one to three orders of magnitude greater than the typical values of a nonlinear part of refractive indices for the orientational Kerr effect and electrostriction in ordinary liquids.[38,39] In the self-focusing case there is a possibility that at a certain power level of light beam diffraction and nonlinearity would balance in such a way that the intensity profile $|A_{o,e}|^2$ remains unchanged on propagation.[41] This is a self-trapping phenomenon[20,38,39,41] which is described by a stable solution of NSE in the form of a homogeneous waveguide channel,[20,39,40] or a spatial soliton.[41] It has the form[18]:

$$A_o = |A_{omax}| \exp i \left[\frac{a_\perp^2 |A_{omax}|^2 \omega^2}{16\pi B c^2 k_o} x' \right] \operatorname{sech} \left[\frac{a_\perp |A_{omax}| \omega}{2\sqrt{2\pi B} c} z' \right] \tag{41}$$

The width w_o of the spatial soliton (41) has the form[18]:

$$w_o = \frac{2\sqrt{2\pi B} c}{a_\perp |A_{omax}| \omega} \tag{42}$$

Consider now the propagation of the extraordinary beam (33), when

$$|A_o| = 0 \tag{43}$$

The diffraction of an extraordinary beam in a medium with a weak optical anisotropy is in general similar to the diffraction of an ordinary one.[42] In liquid crystals the optical anisotropy is much greater than in ordinary optical materials[5,43] which results in the strong dependence of the self-focusing characteristics on the incidence angle of the extraordinary beam. The condition (23) is not met automatically in this case unlike the case of the ordinary beam, and it yields:

$$\operatorname{div} \vec{E}_e = -\frac{\varepsilon_a}{\varepsilon_\perp} \frac{\partial E_{ez}}{\partial z} \tag{44}$$

As a result, the reduced equation for the extraordinary beam contains two types of new terms caused by the optical anisotropy[18]:

1. The term with the first derivative on the transverse coordinate z'' emerges due to the existence of the wave vector component $k_{e\perp}$ normal to the beam vector;

2. The corrections proportional to the anisotropy of the dielectric constant are connected with the deviation of the electric field from transversality.

The term containing the first derivative on the transverse coordinate z'' can be neglected as small in comparison with the term containing the first derivative on the longitudinal coordinate x'':

$$\left| \frac{k_{e\perp}}{k_{e\|}} \frac{\partial A_e}{\partial z''} \right| \ll \left| \frac{\partial A_e}{\partial x''} \right| \tag{45}$$

when the anisotropy angle $(\theta_1 - \theta_e)$ is sufficiently small:

$$\tan(\theta_1 - \theta_e) = \frac{\varepsilon_a}{\varepsilon_{\|}} \frac{\tan\theta_1}{\left[\frac{\varepsilon_\perp}{\varepsilon_{\|}}\tan^2\theta_1 + 1\right]} \ll (k_e w)^{-1} \tag{46}$$

where $k_{e\|}$ is the wave vector component parallel to the beam vector, and w is a transverse dimension of the beam. In SA where the optical anisotropy is much larger than in ordinary crystals, the anisotropy angle can reach a value of 0.1, [18] and in such a case the self-focusing and self-trapping of the extraordinary beam with $k_e \sim 5 \cdot 10^4 cm^{-1}$ are hardly possible for a realistic light intensity.[18] When θ_1 is sufficiently small, the condition (45) can be met, and we obtain the NSE for the extraordinary beam which is similar to the previous case.[18] It has the soliton solution[18]:

$$\begin{aligned} A_e &= |A_{emax}| \exp i \left[\frac{h_e^2 |A_{emax}|^2 \omega^2}{16\pi B l_{e\|} c^2 \left(1 + \frac{\varepsilon_a}{\varepsilon_\perp} e_{ez} \sin\theta_e\right) \sin^2\theta_e} x''\right] \times \\ &\times \operatorname{sech}\left[\frac{h_e |A_{emax}| \omega}{2c\sqrt{2\pi B \left(1 + \frac{\varepsilon_a}{\varepsilon_\perp} e_{ez} \sin\theta_e\right)} \sin\theta_e} z''\right] \end{aligned} \tag{47}$$

The width w_e of the spatial soliton (47) has the form:

$$w_e = \frac{2c\sqrt{2\pi B \left(1 + \frac{\varepsilon_a}{\varepsilon_\perp} e_{ez} \sin\theta_e\right)} \sin\theta_e}{h_e |A_{emax}| \omega} \tag{48}$$

The effective nonlinear part n_{e2}^{eff} of the refractive index of SA may be evaluated as follows:

$$n_{e2}^{eff} = h_e^2 \left[8\pi B \sqrt{\varepsilon_\perp \varepsilon_{\|}} \left(1 + \frac{\varepsilon_a}{\varepsilon_{\|}} e_{ez} \sin\theta_e\right) \sin^2\theta_e\right]^{-1} \tag{49}$$

The comparison of n_{02} and n_{e2}^{eff} shows that in general case both quantities are of the same order of magnitude, but n_{e2}^{eff} strongly depends on the polarization and propagation direction of the extraordinary beam.

Comparing the solutions (41) and (47) one may see that in the case of an arbitrary polarized beam containing both an ordinary component and an extraordinary one each of these components may propagate independently, if the transverse distance between their axes is greater than $(w_o + w_e)/2$. The numerical estimations show that for the typical value of the optical anisotropy of a liquid crystal $(\varepsilon_a/\varepsilon_\perp) \sim 0.3$ [5] and for a comparatively large incidence angle $\theta_o > \pi/4$ the beams would separate after covering a distance comparable with their width. The critical power of the self-trapping $P_{cr} \sim 0.0002 MW$ [18] which can be realized.[39] This power is three orders of magnitude lower than the one for the electrostrictive nonlinearity in benzene or carbone disulfide.[39] The power P of the slab-shaped beam[39] with the dimension in the Y direction $d_y \gg w$ has the form[20]:

$$P = \frac{cd_y}{4\pi}\int_{-\infty}^{\infty} |A(R)|^2 \, dR = \frac{4c^3 B d_y}{a_\perp w_o \omega^2} \tag{50}$$

where R is the transverse coordinate (z' or z'' in our case), and the expression (41) was used for the sake of definiteness. For the critical power $P_{cr} \sim 0.0002\ MW$ and $d_y \sim 10^{-1}$ cm the equation (42) yields $w_o \sim 10^{-2}$ cm. The samples of SA with a thickness of $(10^{-2} \div 6 \cdot 10^{-2})$ cm are known.[9,34] This estimation is also valid for the extraordinary beam in the case of a sufficiently small anisotropy angle.

The self-trapping in the form of a bright surface wave is also possible when the light wave propagates along the interface between an isotropic homogeneous medium and SA cladding.[18] It should be noted that the mechanical instabilities in SA caused by the normal deformations of layers have been investigated experimentally by means of the elastic light scattering.[8] Consequently, we may suppose that the self-focusing and self-trapping of the intensive light beams in the bulk of SA and at the interface between a linear medium and SA due to the light-induced normal deformation of layers would be also observable, if the sufficiently strong pumping is applied.

3.2 The Spatial Self-Modulation of a Light Wave in SA

In the case when the layer normal deformation is absent, and arbitrary polarized light wave propagates in the layer plane the spatial self-phase modulation occurs due to the interaction of components of the optical field which are parallel and perpendicular to the optical axis. These components excite the static grating of the tangential deformation of layers. As a result of the coupling through this grating, each component undergoes spatial phase modulation which influences the polarization of the wave when it propagates in SA. The polarization is characterized by the Stokes parameters[44] which in our case have the form :

$$S_{0,1} = |A_o|^2 \pm |A_e|^2 \tag{51}$$

$$S_2 = 2\,|A_o A_e| \cos\varrho \tag{52}$$

$$S_3 = 2\,|A_o A_e| \sin\varrho \tag{53}$$

$$\varrho = \Delta k_x x + \frac{\omega^2}{c^2}\frac{\varepsilon_a^2 e_x^2}{8\pi K (\Delta k_x)^2 k_{ex} k_{ox}}\left(k_{ox}|A_o|^2 - k_{ex}|A_e|^2\right) x \tag{54}$$

The equations (52)-(54) show that the Stokes parameters are spatially modulated due to the nonlinearity and anisotropy of SA. The spatially inhomogeneous phase difference ϱ (54) consists of two parts. The first term in (54) is caused by the birefringence of SA, and it is similar to the one in any optically uniaxial medium, except that it has a larger magnitude due to the strong optical anisotropy of liquid crystals. The second term is proportional to the intensity of the incident light wave, and it emerges due to the kind of the spatial self-modulation connected with the tangential deformations of the layers. The polarization ellipce of a light wave is characterized by the orientation angle Ψ_{el} and the ellipticity angle χ_{el} in the following way[44]:

$$\tan 2\Psi_{el} = \frac{S_2}{S_1} \tag{55}$$

$$\sin 2\chi_{el} = \frac{S_3}{S_0} \tag{56}$$

The comparison of equations (51)-(54) and equations (55), (56) shows that the polarization ellipce evolves in space, and its form and axis direction depend on the intensity of the wave.

4. THE NONLINEAR WAVE-MIXING IN SA

4.1 The General Approach

We investigated three types of the optical nonlinear wave-mixing in SA which occur due to the new mechanism of optical nonlinearity determined by a layer normal displacement $u(\vec{r}, t)$. [12–17] In the simplest case when two incident light waves are polarized strictly in the incidence plane, or normal to it, a two-wave mixing occurs.[12–15] In general case when two incident light waves have arbitrary polarizations each wave splits into an extraordinary wave and an ordinary one due to the optical anisotropy of SA.[20] As a result, the two-wave mixing transforms into a kind of FWM, which we define as a partly degenerate FWM since there are four fundamental light waves with two different frequencies.[16] The two-wave mixing and the partly degenerate FWM can be characterized as SLS on the second sound which is to some extent analogous to the stimulated Brillouin scattering. When there exist four incident light waves having the essentially different frequencies with the difference between them of an order of magnitude of a second sound frequency a nondegenerate FWM takes place.[17]

In all these situations the following chain of events occurs.[17]

1. The interfering light waves create a dynamic grating of layer displacement $u(\vec{r}, t)$ according to the equation (13). In the case of the two-wave mixing the grating consists of one harmonic.[15] In the case of the partly degenerate

FWM four propagating harmonics with the same frequency and the different wave vectors are excited.[16] In the case of the nondegenerate FWM there exist 6 harmonics with the essentially different frequencies and wave vectors.[17]

2. The fundamental light waves exchange energy and undergo the cross-phase modulation due to the parametric coupling through the light-induced dynamic grating.[12,14–17]

3. The fundamental light waves are scattering on the light-induced dynamic grating and create a spectrum of Brillouin-like harmonics with the Stokes and anti-Stokes frequencies and combination wave vectors.[12,15–17] The polarization of the fundamental waves changes due to the combination of the nonlinearity and anisotropy.[16,17]

Consequently, the total electric field in SA $\vec{E}^{tot}$ can be presented as a sum of a finite number harmonics with SVA[15–17]:

$$\vec{E}^{tot} = \sum \vec{E}_m + \sum \vec{E}'_m + \sum_l \vec{f}_l^S \tag{57}$$

where $\vec{E}_m$ is the field of a fundamental wave, $\vec{E}'_m$ is the additional component of the fundamental wave caused by the combination of anisotropy and nonlinearity, and $\vec{f}_l^S$ is the scattered Brillouin-like harmonic. It is clear that the number of terms in the series (57) depends on the kind of the wave-mixing.

The light absorption by the dynamic grating of the layer displacement can be neglected, since the second sound relaxation time Γ_j^{-1} determined by the viscosity of SA is small in comparison with the time required for the transition of the second sound wave through the region of interaction of the light waves. The dynamic grating turns out to be a sort of a channel providing a total energy transfer between the coupled light waves. In general, SLS on the dynamic grating of the layer displacement can be considered as a steady-state process with the time-independent amplitudes $A(z)$ for the following reasons. The strong energy exchange between the light waves through the slow second sound modes requires a light pulse duration T_p which is much greater than the second sound relaxation time Γ_j^{-1}. The numerical estimations using the values of Δk_j in an interval of $(10^3 \div 5 \cdot 10^4)$ cm^{-1} and the typical values of SA material parameters $\rho \sim 1\ g$ cm^{-3}, $\alpha_i \sim 1$ *Poise* [7,8] show that the relaxation time $\Gamma_j^{-1} \sim (10^{-6} \div 4 \cdot 10^{-10})$ *sec*. This means that even SLS of the nanosecond pulses can be characterized as steady-state one for the dynamic grating with a sufficiently small spatial period Δk_j^{-1}. Consequently, in the further analysis we consider only time-independent SVA. The system possesses one integral of motion including only the light intensities because the second sound modes do not participate directly in the steady-state energy exchange.[15–17]

We substitute the layer displacement $u(\vec{r},t)$ obtained from the equation of motion (13) into the dielectric constant tensor (8), and then combining the total electric field (57) and the nonlinear part ε_{ik}^{NL} of the dielectric constant tensor (8) proportional to the layer deformations we find the nonlinear part $\vec{D}^{NL}$ (22) of the electric induction. It represents a kind of a Fourrier series containing a finite number of harmonics which is determined by the type of wave-mixing process[15–17]:

$$\vec{D}^{NL} = \sum(\vec{D}_l^{NL} \exp i\psi_l + \text{c.c.}) \tag{58}$$

The analysis shows that the amplitudes $\vec{D}_l^{NL}$ are essentially complex.[12,14,16,17] Therefore the amplifcation and the cross-phase modulation of some fundamental waves by other ones due to the complex nonlinear induction are possible.[4] The nonlinear interaction between the light waves is strong only in the case of the phase matching which occurs when the energy and momentum conservation conditions are fulfilled for the frequencies and wave vectors of the coupled waves.[19] In the case of the scattering on the light-induced dynamic grating these conservation conditions are met automatically for the frequencies and wave vectors of the fundamental waves, and therefore in general case the nonlinear induction $\vec{D}^{NL}$ contains the terms which are phase-matched to the fundamental waves and some other terms with the combination frequencies and wave vectors. Consequently, the nonlinear induction gives rise to three types of the essentially nonlinear optical effects.

1. The parametric coupling, amplification and cross-phase modulation are determined by the components of the phase-matched terms $\vec{D}_l^{NL}$ which are parallel to the field of the fundamental waves.

2. The components of the phase-matched terms $\vec{D}_l^{NL}$ which are normal to the fundamental waves field generate the additional components of these fundamental waves. As a result, the fields of all fundamental waves become three-dimensional, while initially some of them were two-dimensional and one-dimensional vectors.

3. The nonlinear terms with combination frequencies and wave vectors create the scattered harmonics (Brillouin-like scattering).

Substituting the total field $\vec{E}^{tot}$ (57) and the nonlinear induction $\vec{D}^{NL}$ (58) into the wave equation (20), taking into account the SVA approximation (25),[19] equating the phase-matched terms and projecting the nonlinear induction on the direction of the field of the fundamental waves we obtain three sets of equations describing the effects mentioned above.[16,17]

1. The first order reduced equations (29) for SVA (28) of the fundamental waves $A_m(z)$. [12,14–17] We do not limit the analysis of the parametric coupling to the constant pumping approximation[19] often used,[2–5] and consider the general case taking into account the depletion of the pumping waves and the saturation of the amplification process.[12,14–17] The number of the reduced equations is equal to the number of the fundamental waves.

2. The wave equations for the additional components $\vec{E}'_m$. These components in general case are neither purely longitudinal, nor purely transverse, and therefore the wave equations sould be solved together with the condition (23).[16,17]

3. The wave equations for the Brillouin-like scattered harmonics $\vec{f}_l^S$.

In principle, the solution of the reduced equations (29) for the moduli and the phases of the SVA (28) with the appropriate boundary conditions provides a full description of a spatial distribution of the intensities and phases of the fundamental waves. However, in general case the explicit solution of the system of these equations is hardly possible. We consider separately the partly degenerate FWM,[16] the two-wave mixing as a particular case of it,[12–15] and nondegenerate FWM.[17] Using the SVA and infinite plane wave approximations[19] we succeeded in calculation of the amplitudes of the coupled waves explicitly in some practically important cases.[12,14–17] In general case the behaviour of the amplitudes has been evaluated qualitatively.[16,17]

It is useful to compare the results obtained for the nondegenerate FWM in SA with the exact theory of the nondegenerate FWM in a non-dissipative isotropic medium with a scalar cubic susceptibility $\chi^{(3)}$ developed in Ref. [45]-[48]. The scalar character and real value of $\chi^{(3)}$ permits a description of a dynamics of a system in terms of the canonical equations for SVA of coupled waves. All phases are varying as a whole in the form of a certain linear combination. As a result, the exact solutions have been obtained in terms of the Jacobian elliptic functions.[45–48] Consequently, the energy exchange depends periodically on the propagation distance. The energy and momentum conservation rules for the frequencies and wave vectors of the coupled waves which are necessary for an effective energy transfer from a pumping wave to amplified waves are to be met simultaneously, which can be provided due to the compensation of an initial wave vector mismatch by the wave vector mismatch caused by the optical Kerr effect.[48] The system has four integrals of motion.

In contrast to the situation considered in Ref. [45]-[48], in our case the cubic susceptibility is a complex tensor[17] which makes the system much more complicated and does not permit an explicit solution. Unlike the case,[45-48] each phase evolves independently.[17] In the case of FWM on the light-induced dynamic grating the conservation laws are met automatically for all fundamental waves, and the wave vector mismatch vanishes. The system considered in our case has only one integral of motion because the direct energy exchange between the optical field and the second sound is negligible. Such an approximation is valid, if the dissipation length of a second sound mode

$$L_D = s_0 \tau_s \tag{59}$$

is small in comparison with the excitation length[25] of a virtual second sound mode L_E. In the case of the nondegenerate FWM in SA there exist 6 excitation lengths which can be also defined as the correlation lengths for each pair of the coupled light waves E_m and E_n. It has been shown[17] that in the case of the light-induced dynamic grating

$$\frac{L_D}{L_E} \ll 1 \tag{60}$$

Consequently, the second sound modes are passive, or "slaved", and the scale separation exists between the dissipation and excitation processes.[25] The light-induced dynamic grating plays a role of an elastic channel for the energy transfer from the pumping wave with the largest frequency to the other waves. The energy exchange occurs on a distance of an order of magnitude of the excitation length L_E, and it is non-reciprocal, unlike the situation in the conservative system.[48]

4.2 The Partly Degenerate FWM

Consider two incident light waves propagating from a free semi-space $z < 0$ to SA filling a semi-space $z > 0$:

$$\vec{E}^I_{1,2} = \vec{e}^I_{1,2}\left[A^I_{1,2}\exp i\left(\vec{k}^I_{1,2}\vec{r} - \omega t\right) + \text{c.c.}\right] \tag{61}$$

$$(k^I_{1,2})^2 = \frac{\omega^2_{1,2}}{c^2} \tag{62}$$

where the polarization unit vectors $\vec{e}^I_{1,2}$ are assumed to be three - dimensional, the frequencies $\omega_{1,2}$ are assumed to be close:

$$\Delta\omega = \omega_1 - \omega_2 \ll \omega_1 \tag{63}$$

and we choose for the sake of definiteness that

$$\omega_1 > \omega_2 \tag{64}$$

We define the incidence plane of the wave $\vec{E}_1^I$ as the XZ plane. Such a choice is possible, since SA possess the symmetry D_∞ [7,8] which permits any rotation around the optical axis coinciding with the Z axis. In this geometry four waves would propagate in SA[20]:

$$\vec{E}_1^{o,e} = e^{\vec{o},e}{}_1 \left[A_1^{o,e}(z) \exp i \left(\vec{k}_1^{o,e}\vec{r} - \omega_1 t\right) + \text{c.c.}\right] \tag{65}$$

$$\vec{E}_2^{o,e} = e^{\vec{o},e}{}_2 \left[A_2^{o,e}(z) \exp i \left(\vec{k}_2^{o,e}\vec{r} - \omega_2 t\right) + \text{c.c.}\right] \tag{66}$$

It is easy to show that the extraordinary waves $\vec{E}_{1,2}^e$ possess the components parallel to the optical axis and the ones normal to it. The ordinary waves $\vec{E}_{1,2}^o$ do not possess the components parallel to the optical axis. Both ordinary waves are transverse. The system of the light waves coupled through the dynamic grating possesses an integral of motion including only the light intensities because the second sound modes do not participate directly in the steady-state energy exchange. The integral of motion has the form[16]:

$$\frac{c^2}{\omega_1^2}\left(l_1^o |A_1^o|^2 + l_1^e |A_1^e|^2\right) + \frac{c^2}{\omega_2^2}\left(l_2^o |A_2^o|^2 + l_2^e |A_2^e|^2\right) = I_0 = \text{const} \tag{67}$$

It is instrumental to introduce the dimensionless variables

$$W_{1,2}^{o,e} = \frac{c^2 l_{1,2}^{o,e} \left|A_{1,2}^{o,e}\right|^2}{\omega_{1,2}^2 I_0} \tag{68}$$

Substituting (68) into (67) we obtain

$$W_1^o + W_1^e + W_2^o + W_2^e = 1 \tag{69}$$

The calculation of the explicit solution of the system of the reduced equations in general case is hardly possible, and we investigate the qualitative behaviour of the dimensionless intensities $W_{1,2}^{o,e}$ and phases $\gamma_{1,2}^{o,e}$. The system has the formal solution in the integral form[16]:

$$W_1^{o,e} = W_1^{o,e}(0) \exp\left[-\int_0^z \left(\beta_{3,2} W_2^{o,e} + \beta_{4,1} W_2^{e,o}\right) dz'\right] \tag{70}$$

$$W_2^{o,e} = W_2^{o,e}(0) \exp\left[\int_0^z \left(\beta_{3,2} W_1^{o,e} + \beta_{1,4} W_1^{e,o}\right) dz'\right] \tag{71}$$

$$\gamma_1^{o,e} - \gamma_1^{o,e}(0) = \int_0^z \left[-\frac{1}{2}\left(\delta_{3,2} W_2^{o,e} + \delta_{4,1} W_2^{e,o}\right) dz'\right] \tag{72}$$

$$\gamma_2^{o,e} - \gamma_2^{o,e}(0) = \int_0^z \left[-\frac{1}{2}\left(\delta_{3,2} W_1^{o,e} + \delta_{1,4} W_1^{e,o}\right) dz'\right] \tag{73}$$

The coupling constants β_j and δ_j have the form :

$$\beta_j = \frac{\omega_1^2\omega_2^2 I_0}{c^4 d_j}\frac{\Delta\omega h_j^2(\Delta k_{j\perp})^2\Gamma_j}{4\pi\rho(\Delta k_j)^2\,|G_j|^2} > 0 \tag{74}$$

$$\delta_j = \frac{\omega_1^2\omega_2^2 I_0}{c^4 d_j}\frac{h_j^2(\Delta k_{j\perp})^2}{4\pi\rho(\Delta k_j)^2\,|G_j|^2}\left[(\Delta\omega)^2 - \Omega_j^2\right] \tag{75}$$

where

$$d_1 = l_1^e l_2^o, \quad d_2 = l_1^e l_2^e, \quad d_3 = l_1^o l_2^o, \quad d_4 = l_1^o l_2^e \tag{76}$$

the quantities $l_{1,2}^{o,e}$ are determined as follows

$$l_m = k_{mz}^o, \quad \text{or} \quad k_{mz}^e\left[1 - e_{mz}^e\frac{(\vec{k}_m^e\vec{e}^e{}_m)}{k_{mz}^e}\right]$$

for the ordinary and the extraordinary waves, respectively, and

$$\begin{aligned}
h_1 &= a_\perp\Delta k_{1z}e_{1x}^e e_{2x}^o - \varepsilon_a(\Delta k_{1x}e_{1z}^e e_{2x}^o + \Delta k_{1y}e_{1z}^e e_{2y}^o)\\
h_2 &= a_\perp\Delta k_{2z}e_{1x}^e e_{2x}^e + a_{||}\Delta k_{2z}e_{1z}^e e_{2z}^e - \\
&\quad \varepsilon_a\left[\Delta k_{2x}(e_{1x}^e e_{2z}^e + e_{1z}^e e_{2x}^e) + \Delta k_{2y}e_{1z}^e e_{2y}^e\right]\\
h_3 &= a_\perp\Delta k_{3z}e_{2y}^o\\
h_4 &= a_\perp\Delta k_{4z}e_{2y}^e - \varepsilon_a\Delta k_{4y}e_{2z}^e
\end{aligned} \tag{77}$$

The denominator of the second sound Green function Fourrier transform has the form:

$$G_j = (\Delta\omega)^2 - \Omega_j^2 + i\Delta\omega\Gamma_j \tag{78}$$

The quantities Ω_j and Γ_j have the meaning of the frequency and the time decay constant of the second sound, respectively:

$$\Omega_j^2 = s_0^2\frac{(\Delta k_{j\perp}\Delta k_{jz})^2}{(\Delta k_j)^2} \tag{79}$$

$$\Gamma_j = \frac{1}{\rho}\left[\alpha_1\left(\frac{\Delta k_{j\perp}\Delta k_{jz}}{\Delta k_j}\right)^2 + \frac{1}{2}(\alpha_4 + \alpha_{56})(\Delta k_j)^2\right] \tag{80}$$

The wave vectors $\Delta\vec{k}_j$ of the dynamic grating represent the differences of the fundamental wave vectors $\vec{k}_j$:

$$\begin{aligned}
\Delta\vec{k}_1 &= \vec{k}_1^e - \vec{k}_2^o\\
\Delta\vec{k}_2 &= \vec{k}_1^e - \vec{k}_2^e\\
\Delta\vec{k}_3 &= \vec{k}_1^o - \vec{k}_2^o\\
\Delta\vec{k}_4 &= \vec{k}_1^o - \vec{k}_2^e
\end{aligned} \tag{81}$$

and

$$(\Delta k_{j\perp})^2 = (\Delta k_{jx})^2 + (\Delta k_{jy})^2 \tag{82}$$

Taking into account the conditions (67)-(69) and (74) we obtain from the equations (70) and (71):

$$z \to \infty \quad W_1^{o,e} \to 0, \quad W_2^o + W_2^e \to 1 \tag{83}$$

The relationship (83) shows that the energy transfer from the pair of waves with the greater frequency ω_1 to the pair of waves with the lower frequency ω_2 occurs. The influence of the cross-phase modulation on the parametric process is determined by the ratio of the coupling constants β_j and δ_j. According to the condition (74) the constants β_j are positive definite while δ_j may be positive as well as negative which corresponds to the behaviour of SA as focusing, or defocusing medium, respectively.[20] The resonance case when

$$(\Delta\omega)^2 = \Omega_j^2 \tag{84}$$

is the most favourable one for the strong coupling since the energy transfer occurs at almost constant phases.[16] Consider the practically important case when each of the incident light waves (61) has mainly one type of polarization, and their components with other polarization are much less than the main ones. We investigate the behaviour of these small components and their influence on the main components. Let, for example, the pumping wave $\vec{E}_1^I$ is mainly polarized in the incidence plane, while the signal wave $\vec{E}_2^I$ is mainly polarized normal to its incident plane. In this case the dimensionless variables $W_{1,2}^{o,e}$ (68) obey the conditions:

$$W_1^e \gg W_1^o, \quad W_2^o \gg W_2^e \tag{85}$$

The intensities W_1^e and W_2^o can be expanded into a series because all intensities are finite and sufficiently smooth at large distances z, as it has been shown previously[16]:

$$W_1^e = W_{10}^e + W_{11}^e + \dots, \quad |W_{11}^e| \ll W_{10}^e \tag{86}$$

$$W_2^o = W_{20}^o + W_{21}^o + \dots, \quad |W_{21}^o| \ll W_{20}^o \tag{87}$$

Substituting the expansions (86) and (87) into the general system of the reduced equations we obtained the chain of coupled equations[16] which have in the first approximation a separate integral of motion

$$J_1 = W_{10}^e + W_{20}^o = W_1^e(0) + W_2^o(0) < 1 \tag{88}$$

and the solutions[16]:

$$W_{10}^{e} = \frac{J_1}{2}\left[1 - \tanh(\eta - \eta_0)\right] \tag{89}$$

$$W_{20}^{o} = \frac{J_1}{2}\left[1 + \tanh(\eta - \eta_0)\right] \tag{90}$$

The system of equations of the second approximation has another integral of motion:

$$J_2 = W_{11}^{e} + W_{21}^{o} + W_1^{o} + W_2^{e} = \text{const} \tag{91}$$

and the solutions[16]:

$$W_2^{e} = W_2^{e}(0)\left[\cosh(\eta_0)\exp(\eta)\text{sech}(\eta - \eta_0)\right]^{b_1} \tag{92}$$

$$W_1^{o} = W_1^{o}(0)\left[\cosh(\eta_0)\exp(-\eta)\text{sech}(\eta - \eta_0)\right]^{b_2} \tag{93}$$

where

$$b_{1,2} = \frac{\beta_{2,3}}{\beta_1} \tag{94}$$

and the dimensionless variable η has the form:

$$\eta = \frac{\beta_1}{2} z$$

The quantity z_0 has the meaning of a coordinate of a critical point where the intensities of the pumping and signal waves are equal.

$$z_0 = \frac{1}{\beta_1}\ln\left[\frac{W_1^{e}(0)}{W_2^{o}(0)}\right] \tag{95}$$

It exists, if

$$W_1^{e}(0) > W_2^{o}(0)$$

It is seen from the relationships (92) and (93) that the ordinary component of the pumping wave vanishes as $\eta \to \infty$, while the extraordinary component of the signal wave increases and reaches the saturation level at sufficiently large $\eta \gg \eta_0$:

$$\eta \to \infty, \qquad W_1^{o} \to 0, \quad (W_1^{o})_{max} = W_1^{o}(0) \tag{96}$$

$$\eta \to \infty, \quad W_2^{e} \to W_2^{e}(0)\left[1 + \frac{W_1^{e}(0)}{W_2^{o}(0)}\right]^{b_2} > W_2^{e}(\eta) \tag{97}$$

The small corrections W_{11}^{e} and W_{21}^{o} have the form[16]:

$$\begin{aligned} W_{11}^{e} &= \left[\text{sech}(\eta - \eta_0)\right]^2 \int_0^{\eta} d\eta' \left[\cosh(\eta' - \eta_0)\right]^2 \left[1 - \tanh(\eta' - \eta_0)\right] \times \\ &\quad \times \left[W_1^{o} + W_2^{e}(1 - b_1) - J_2\right] \end{aligned} \tag{98}$$

$$\begin{aligned} W_{21}^{o} &= \left[\text{sech}(\eta - \eta_0)\right]^2 \int_0^{\eta} d\eta' \left[\cosh(\eta' - \eta_0)\right]^2 \left[1 + \tanh(\eta' - \eta_0)\right] \times \\ &\quad \times \left[J_2 - W_2^{e} - W_1^{o}(1 - b_2)\right] \end{aligned} \tag{99}$$

$$J_2 = W_1^{o}(0) + W_2^{e}(0), \quad J_1 + J_2 = 1 \tag{100}$$

The solutions (92), (93), (98) and (99) satisfy the conservation law (91) automatically which can be proved immediately[16]:

$$W_1^o + W_2^e + W_{11}^e + W_{21}^0 = W_1^o + W_2^e + [\mathrm{sech}(\eta - \eta_0)]^2 \times \times \int_0^\eta d\eta' \frac{d}{d\eta'} \left[[\cosh(\eta' - \eta_0)]^2 (J_2 - W_1^o - W_2^e) \right] \equiv J_2 \tag{101}$$

The explicit calculation of the integrals (98) and (99) is hardly possible. However, we evaluated the lower and the upper limits of these expressions using the relationships (92), (93), (96) and (97) and assuming without the loss of generality that

$$b_{1,2} < 1 \tag{102}$$

The analysis shows that the corrections W_{11}^e and W_{21}^o are finite, small, and they satisfy the conservation law (91) for all η. [16] The system is stable with respect to the thickness of SA sample and to the pumping intensity.[16]

The phases $\gamma_1^{o,e}$ of the pumping waves $\vec{E}_1^{o,e}$ rapidly increase with $\eta \to \pm\infty$ which means that the depletion of the pumping waves is accompanied by the oscillations of their amplitudes.[16] On the contrary, the phase $\gamma_2^{o,e}$ of the signal waves $\vec{E}_2^{o,e}$ reach the constant value at sufficiently large η, and the saturation of the amplification process occurs at almost constant phases.[16]

The Brillouin-like scattered harmonics $\vec{f}_l^S$ with the combination frequencies and wave vectors result from the coupling of the fundamental waves (65) and (66) with the field-induced dynamic grating. They are governed by the terms in the nonlinear induction (58) which are not phase-matched to the fundamental modes (65) and (66). These harmonics evolve according to the wave equation

$$\mathrm{rot\ rot} \vec{f}_l^S + \frac{1}{c^2} \frac{\partial^2}{\partial t^2} \left[\varepsilon_\perp \left(f_{lx}^S \vec{x} + f_{ly}^S \vec{y} \right) + \varepsilon_\parallel f_{lz}^S \vec{z} \right] = -\frac{1}{c^2} \frac{\partial^2}{\partial t^2} \left(\vec{D}_l^{NL} \exp i\psi_l \right) \tag{103}$$

The combination frequencies and wave vectors do not satisfy the corresponding dispersion relations,[20] and therefore the scattered harmonics consist only of the inhomogeneous solution which is driven by the nonlinear polarization in the right-hand side of the wave equation (103). They have the form:

$$\vec{f}_l^s = \vec{F}_l^s \exp i\psi_l + \mathrm{c.c.} \tag{104}$$

These harmonics are essentially weak in comparison with the fundamental modes.[19] The spectrum of the scattered harmonics contains 12 terms with the following Stokes and anti-Stokes frequencies ω_S and ω_A, respectively:

$$\begin{aligned} \omega_S &= 2\omega_2 - \omega_1 = \omega_2 - \Delta\omega \\ \omega_A &= 2\omega_1 - \omega_2 = \omega_1 + \Delta\omega \end{aligned} \tag{105}$$

They have the following phases[16]:

$$\begin{gathered}\left[(2\vec{k}_1^e - \vec{k}_2^{o,e})\vec{r} - \omega_A t\right], \qquad \left[(2\vec{k}_1^o - \vec{k}_2^{o,e})\vec{r} - \omega_A t\right] \\ \left[(\vec{k}_1^e + \vec{k}_1^o - \vec{k}_2^{o,e})\vec{r} - \omega_A t\right], \qquad \left[(\vec{k}_2^o + \vec{k}_2^e - \vec{k}^{o,e})\vec{r} - \omega_S t\right] \\ \left[(2\vec{k}_2^e - \vec{k}_1^{o,e})\vec{r} - \omega_S t\right], \qquad \left[(2\vec{k}_2^o - \vec{k}_1^{o,e})\vec{r} - \omega_S t\right] \end{gathered} \tag{106}$$

Besides that there are 8 terms with the fundamental frequencies $\omega_{1,2}$ and with the combination wave vectors:

$$\begin{gathered}\left[(\vec{k}_2^e - \vec{k}_2^o + \vec{k}_1^{o,e})\vec{r} - \omega_1 t\right], \qquad \left[(\vec{k}_2^o - \vec{k}_2^e + \vec{k}_1^{o,e})\vec{r} - \omega_1 t\right] \\ \left[(\vec{k}_1^e - \vec{k}_1^o + \vec{k}_2^{o,e})\vec{r} - \omega_2 t\right], \qquad \left[(\vec{k}_1^o - \vec{k}_1^e + \vec{k}_2^{o,e})\vec{r} - \omega_2 t\right] \end{gathered} \tag{107}$$

These terms are specific for the partly degenerate FWM. The four terms with the fundamental phases $(\vec{k}_1^{o,e}\vec{r} - \omega_1 t)$ and $(\vec{k}_2^{o,e}\vec{r} - \omega_2 t)$ are also doubly degenerate since only two different frequencies exist: ω_1 and ω_2 . The total number of the terms is consequently equal to 32, including 24 terms with essentially different phase factors: 4 phase-matched terms and 20 scattered harmonics, as it was mentioned above. The explicit form of the amplitudes $\vec{F}_l^s$ is too involved, and we do not present them here. However, we can conclude using the relationships (13), (22), (68), (83) and (103) that all harmonics are spatially localized, and their amplitudes vanish at infinity:

$$z \to \infty, \quad |F_l^s| \to 0 \tag{108}$$

The additional components driven by the nonlinear part of the electric induction $\vec{D}^{NL}$ have been calculated explicitly.[16] Both anisotropy of the linear part of ε_{ik} and the nonlinearity are essential for the existence of the components $\vec{f}_1^o$, f_{1y}^e and f_{2z}^o. The amplitudes of the additional components are proportional to $|A_1^{o,e}|$, and therefore they are spatially localized.

$$z \to \infty, \quad |f_1^o|, \quad \left|f_{1y}^e\right|, \quad |f_{2z}^o| \to 0 \tag{109}$$

4.3 The Two-Wave Mixing

Consider the particular case when the two coupled waves are polarized strictly in the incidence plane, or normal to it. In the former case the waves propagate as extraordinary ones, in the latter case they propagate as ordinary ones.[20] These two cases differ by the form of the coupling constants (77).[12–15] The reduced equations in this case can be solved explicitly. Let, for example, there exists the extraordinary wave $\vec{E}_1^e$ and the ordinary wave $\vec{E}_2^o$. Their interference gives rise to the dynamic grating consisting of only one harmonic. The conservation law yields:

$$W_1^e(z) + W_2^o(z) = W_1^e(0) + W_2^o(0) = 1 \tag{110}$$

The solution has the form:

$$W_1^e = \frac{W_1^e(0)}{W_2^o(0)} \left[\frac{W_1^e(0)}{W_2^o(0)} + \exp(\beta_1 z) \right]^{-1} \tag{111}$$

$$W_2^o = \left[\frac{W_1^e(0)}{W_2^o(0)} + \exp(\beta_1 z) \right]^{-1} \exp(\beta_1 z) \tag{112}$$

If the pumping wave intensity $W_1^e(0)$ at the entrance of SA is greater than the signal wave intensity $W_2^o(0)$, we obtain substituting the expression (95) into (111) and (112) :

$$W_1^e = \frac{1}{2} [1 - \tanh(\eta - \eta_0)] \tag{113}$$

$$W_2^o = \frac{1}{2} [1 + \tanh(\eta - \eta_0)] \tag{114}$$

Substituting the expressions (113) and (114) into the equations (72) and (73) we find the phases:

$$\gamma_1^e - \gamma_1^e(0) = \frac{\delta_1}{2\beta_1} \ln \left[\frac{\cosh(\eta_0) \exp(-\eta)}{\cosh(\eta - \eta_0)} \right] \tag{115}$$

$$\gamma_2^o - \gamma_2^o(0) = \frac{\delta_1}{2\beta_1} \ln \left[\cosh(\eta_0) \exp(-\eta) \cosh(\eta - \eta_0) \right] \tag{116}$$

So far we neglected the light absorption in SA. In general, the optical transmission losses in liquid crystals are caused by the absorption and light scattering on the orientational fluctuations.[1] The off-resonance light absorption in liquid crystals is small $\sim (10^{-2} \div 10^{-1})$ cm^{-1}. [1] The optical transmission losses due to the strong light scattering on the orientational fluctuations are typical for NLC, while in SA this mechanism of optical losses is considerably less manifested because of the higher degree of molecules ordering.[1] Consequently, the negligence of the losses used in our analysis is valid, especially in the case when two strong incident waves interact.[19] Nevertheless, it is useful to evaluate the threshold of the simultaneous excitation of the second sound wave

$$u = U(z) \exp i(\vec{k}_s \vec{r} - \Omega t) + \text{c.c.} \tag{117}$$

and of the scattered Stokes wave $\vec{E}_2^e$ (66) by the strong pumping wave $\vec{E}_1^e$ (65) in the process analogous to the stimulated Brillouin scattering on an ordinary sound when at the first stage only the strong wave $\vec{E}_1^e$ exists.[49,50] The absorption is taken into account by means of the imaginary part of the diagonal components $\varepsilon'_\perp$ and $\varepsilon'_\parallel$ of the dielectric constant tensor (8).[20] The excitation of the wave E_2^e and the second sound wave $u(\vec{r}, t)$ occurs, if[13]

$$\frac{|A_1^e|^2}{B} > \frac{4\pi k_{sz}^2 \Gamma_2 \left[\varepsilon'_\perp (e_{2x}^e)^2 + \varepsilon'_\parallel (e_{2z}^e)^2\right]}{h_{2e}^2 \Omega} \tag{118}$$

The inequality (118) is similar to the condition of the stimulated Brillouin scattering on an ordinary sound.[49,50] For SA we can neglect the losses caused by the scattering on the orientational fluctuations.[1] The numerical estimations show that the threshold intensity value

$$\mathcal{P} \sim \frac{c}{4\pi} |A_{1\text{thr}}^e|^2 \sim 1\ MW\ \text{cm}^{-2}$$

which is slightly less than the intensity threshold for an ordinary sound excitation in organic liquids such as n-hexane, carbon disulfide etc..[49]

For the typical values of the material parameters of SA[1,7,26] the following inequalities take place[13]:

$$\begin{aligned} \frac{\Gamma_2 k_{sz} k_s^2}{\Omega k_{sx}^2} &\gg \frac{\omega_2^2 \left[\varepsilon'_\perp (e_{2xe})^2 + \varepsilon'_\parallel (e_{2z}^e)^2\right]}{l_2^e c^2} \\ \frac{\Gamma_2}{\Omega} &\gg \frac{|A_1^e|^2}{B} \end{aligned} \tag{119}$$

Taking into account these conditions we obtain the amplitude gain coefficient[13]:

$$g_2 \simeq \frac{|A_1^e|^2 \omega_2^2 \Omega h_{2e}^2}{8\pi B l_2^e c^2 \Gamma_2 k_{sz}^2} \tag{120}$$

Consider finally the stimulated scattering of two light waves

$$\vec{E}_1 = \vec{e}_1 \left[A_1(x) \exp i(k_{1x} x + k_{1y} y - \omega_1 t) + \text{c.c.}\right] \tag{121}$$

$$E_2 = E_z = A_2(x) \exp i(k_{2x} x + k_{2y} y - \omega_2 t) + \text{c.c.} \tag{122}$$

propagating in a layer plane of a planary oriented[7,8] SA on the so-called undulation mode.[14] The X axis is chosen to be normal to the interface $x = 0$ between a linear medium ($x < 0$) and SA ($x > 0$). In such a case the second sound cannot be excited, and the normal deformation of a layer vanishes according to the equation (16). The overdamped undulation mode

$$u = U(x) \exp i(\Delta \vec{k} \vec{r} - \Delta \omega t) + \text{c.c.} \tag{123}$$

is determined by the equation of motion (17). The form of the solution for the field amplitudes is analogous to the two-wave mixing on the second sound (113), (114), and it has been obtained.[14] However, SLS on the overdamped undulation mode (123) lacks a resonant character. The comparison of the gain coefficients β_u and β_2^r shows[12,14] that in the case of small frequency difference

$$\Delta\omega \ll \Gamma_2 \sim \Omega_2 \tag{124}$$

the amplification is stronger in the case of SLS on the undulation mode, and it occurs at the almost constant phases. The case when

$$\Delta\omega \sim \Gamma_2 \sim \Omega_2 \tag{125}$$

is favourable for both kinds of SLS.[12,14] Finally, the condition

$$\Delta\omega \gg \Gamma_2 \sim \Omega_2 \tag{126}$$

leads to the small amplification and strong cross-phase modulation in both situations considered since it is impossible to satisfy the resonance condition (84) for the second sound, and, on the other hand, the gain coefficient β_u decreases as $(\Delta\omega)^{-3}$.[14]

4.4 The Four-wave Mixing in SA

Consider a nondegenerate FWM in SA when four fundamental light waves have close frequencies with the difference

$$\Delta\omega_{mn} = \omega_m - \omega_n \sim \frac{s_0}{c}\omega_m \ll \omega_m \tag{127}$$

For the sake of definiteness we assume that

$$\omega_1 < \omega_2 < \omega_3 < \omega_4 \tag{128}$$

It turned out that this case is essentially different from the one of partly degenerate FWM.[17] Namely, the light wave with the lowest frequency is amplified up to a saturation level, the light wave with the highest frequency is depleted, while two waves with the intermediate frequencies are compressed in space forming the soliton-like envelopes.[17] Suppose that four light waves propagate from a free semi-space $z < 0$ into SA filling a semi-space $z > 0$. SA is homeotropically oriented,[7,8] and its optical axis coincides with the Z axis. The X and Y axes are chosen to be in a layer plane, as usual. Using the infinite plane wave and SVA approximations[19] we write the electric fields of the four fundamental waves in SA in the following form:

$$\vec{E}_m = \vec{e}_m \left[A_m(z) \exp i(\vec{k}_m\vec{r} - \omega_m t) + \text{c.c.}\right], \quad m = 1, \ldots, 4 \tag{129}$$

In general case an arbitrary polarized light wave splits into an ordinary wave and an extraordinary one.[20] As a result, the eight-wave mixing would occur instead of FWM. This case is not considered. We assume that all fundamental waves are either polarized normal to an incidence plane and propagate as ordinary waves, or they are polarized in an incidence plane and, consequently, propagate as extraordinary ones.[20] In the first case they have polarization unit vectors

$$\vec{e^o}_m = \vec{e^o}_{m\perp} = (e_{mx}, e_{my}, 0) \tag{130}$$

and the dispersion relation[20]:

$$(k^o_m)^2 = \frac{\omega_m^2}{c^2}\varepsilon_\perp \tag{131}$$

In the second case the polarization unit vectors $\vec{e^e}_m$ are three-dimensional:

$$\vec{e^e}_m = (\vec{e^e}_{m\perp}, e^e_{mz}) \tag{132}$$

and the wave vectors $\vec{k}^e_m$ obey the dispersion relation[20]:

$$\frac{(k^e_{m\perp})^2}{\varepsilon_{\|}} + \frac{(k^e_{mz})^2}{\varepsilon_\perp} = \frac{\omega_m^2}{c^2} \tag{133}$$

where

$$\vec{k}^e_{m\perp} = k^e_{mx}\vec{x} + k^e_{my}\vec{y}$$

We consider separately the cases of the interaction of the extraordinary and ordinary waves. They differ by the form of the coupling constants h_{mn}. First consider the coupling of the extraordinary waves. The dynamic grating of the layer displacement consisting of 6 harmonics has the form[17]:

$$u(\vec{r}, t) = \sum_{m,n,m\neq m} U_{mn} \exp i(\Delta\vec{k}_{mn} - \Delta\omega_{mn}t) \tag{134}$$

where

$$\Delta\vec{k}_{mn} = \vec{k}_m - \vec{k}_n \tag{135}$$

$$U_{mn} = \frac{ih_{mn}(\Delta k_{mn\perp})^2}{4\pi\rho G_{mn}(\Delta k_{mn})^2} A_m A_n^* \tag{136}$$

$$\begin{aligned} h_{mn} = {} & \left[a_\perp(\vec{e}_{m\perp}\vec{e}_{n\perp}) + a_{\|}(e_{mz}e_{nz})\right]\Delta k_{mnz} - \\ & -\varepsilon_a\left[e_{mz}(\Delta\vec{k}_{mn}\vec{e}_{n\perp}) + e_{nz}(\Delta\vec{k}_{mn\perp}\vec{e}_{m\perp})\right] \end{aligned} \tag{137}$$

$$G_{mn} = (\Delta\omega_{mn})^2 - \Omega^2_{mn} + i\Delta\omega_{mn}\Gamma_{mn} \tag{138}$$

$$\Omega^2_{mn} = s_0^2\left(\frac{\Delta k_{mn\perp}\Delta k_{mnz}}{\Delta k_{mn}}\right)^2 \tag{139}$$

$$\Gamma_{mn} = \frac{1}{\rho}\left[\alpha_1\left(\frac{\Delta k_{mn\perp}\Delta k_{mnz}}{\Delta k_{mn}}\right)^2 + \frac{(\alpha_4 + \alpha_{56})}{2}(\Delta k_{mn})^2\right] \tag{140}$$

The coupling constants h_{mn} depend on the polarization of the waves. In the case of the mixing of ordinary waves h^{o}_{mn} takes the form:

$$h^{o}_{mn} = a_{\perp} \Delta k_{mnz} (\vec{e}_{m\perp} \vec{e}_{n\perp}) \tag{141}$$

The contribution of the static layer deformations

$$\left(\frac{\partial u_m}{\partial z} \right)_{stat} \sim \frac{a_{\perp}}{4\pi B} |A_m|^2 \tag{142}$$

can be neglected, as small in comparison with the deformations of the dynamic grating (134).[17]

The detailed analysis of the system of equations describing FWM[17] shows that the parametric amplification with saturation of only one wave E_1 occurs, while three other waves $E_{2,3,4}$ undergo total depletion:

$$z \to \infty, \quad W_1 \to 1, \quad W_{2,3,4} \to 0 \tag{143}$$

The intensities of the waves $E_{2,3}$ with the intermediate frequencies form the spatially localized soliton-like states, if the pumping wave E_4 at the input $z = 0$ is sufficiently strong. In the excitation interval

$$\min(z_{02}, z_{03}) > z > 0 \tag{144}$$

three waves $E_{1,2,3}$ are amplified. Here z_{02} and z_{03} are the coordinates of the points of maximum of $W_{2,3}$. The solutions $W_{1,2,3,4}$ are non-periodical and stable with respect to a sample thickness and a pumping intensity.[17]

The behaviour of the phases γ_m is analogous to the situation considered in the previous section: each phase evolves independently. If for all m, n

$$(\Delta\omega_{mn})^2 > \Omega^2_{mn} \tag{145}$$

then all phase shifts are negative, i.e. the medium behaves as a defocusing one.[19,20] In the opposite case

$$(\Delta\omega_{mn})^2 < \Omega^2_{mn} \tag{146}$$

all phase shifts are positive, and SA is a focusing medium.[19,20]

Consider the important case when the pumping wave $\vec{E}_4$ and the signal wave $\vec{E}_1$ are much stronger than the idler waves $\vec{E}_{2,3}$:

$$W_{1,4} \gg W_{2,3} \tag{147}$$

The conservation law[17]

$$\sum_{m=1}^{4} l_m \left(\frac{\omega_m}{c}\right)^{-2} |A_m|^2 = \text{const} = I_0 \tag{148}$$

expressed through the dimensionless variables W_m takes the form[17]:

$$W_m = \frac{1}{I_0} l_m \left(\frac{\omega_m}{c}\right)^{-2} |A_m|^2, \quad \sum_{m=1}^{4} W_m = 1 \tag{149}$$

The conditions (143) and (149) permit the following expansion:

$$\begin{aligned} W_1 &= W_{10} + W_{11} + \ldots \\ W_4 &= W_{40} + W_{41} + \ldots \\ W_{10} &\gg |W_{11}|, \quad W_{40} \gg |W_{41}| \end{aligned} \tag{150}$$

In this case the explicit solution can be obtained which has the form[17]:

$$W_{10,40} = \frac{J_1}{2}\left[1 \pm \tanh \frac{\beta_{41} J_1}{2}(z - z_1)\right] \tag{151}$$

$$W_2 + W_3 + W_{11} + W_{41} = \text{const} = J_2 \tag{152}$$

$$W_2 = W_2(0) \exp(a_1 \eta) \left[\cosh(\eta_1) \text{sech}(\eta - \eta_1)\right]^{c_1} \tag{153}$$

$$W_3 = W_3(0) \exp(a_2 \eta) \left[\cosh(\eta_1) \text{sech}(\eta - \eta_1)\right]^{c_2} \tag{154}$$

where

$$\begin{aligned} J_1 &= W_1(0) + W_4(0) \\ \eta &= \frac{\beta_{41} J_1}{2} z, \quad z_1 = \frac{1}{\beta_{41} J_1} \ln\left[\frac{W_4(0)}{W_1(0)}\right] \\ a_1 &= \frac{\beta_{42} - \beta_{21}}{\beta_{41}}, \quad a_2 = \frac{\beta_{43} - \beta_{31}}{\beta_{41}} \\ c_1 &= \frac{\beta_{42} + \beta_{21}}{\beta_{41}}, \quad c_2 = \frac{\beta_{43} + \beta_{31}}{\beta_{41}} \end{aligned} \tag{155}$$

and the coupling constants β_{mn} have the form[17]:

$$\beta_{mn} = \frac{\omega_m^2 \omega_n^2 I_0 h_{mn}^2 \Delta\omega_{mn} \Gamma_{mn} (\Delta k_{mn\perp})^2}{4\pi \rho c^4 l_m l_n |G_{mn}|^2 (\Delta k_{mn})^2} \tag{156}$$

Each coupling constant β_{mn} represents the contribution of the elementary two-wave mixing process in the FWM process. The coupling constants β_{mn} play a role of the gain coefficients, and their moduli reach maximal values in the case of the resonance:

$$(\Delta\omega_{mn})^2 = \Omega_{mn}^2 \tag{157}$$

In the resonance case (157) β_{mn} has the form[17]:

$$|\beta^{r}_{mn}| = \frac{\omega_m^2 \omega_n^2 I_0 h_{mn}^2 |\Omega_{mn}|}{4\pi B l_m l_n c^4 \Gamma_{mn} (\Delta k_{mnz})^2} \sim \sim \frac{\omega_m \mathcal{P} \varepsilon_a^2 |\Omega_{mn}|}{B c^2 \Gamma_{mn} \sqrt{\varepsilon_\perp \varepsilon_\parallel}} \tag{158}$$

The small corrections are[17]:

$$W_{11} = [\mathrm{sech}(\eta - \eta_1)]^2 \int_0^\eta [\cosh(\eta' - \eta_1)]^2 [1 + \tanh(\eta' - \eta_1)] \times \times [\beta_{41} J_2 + W_2(\beta_{21} - \beta_{41}) + W_3(\beta_{31} - \beta_{41})] \frac{1}{\beta_{41}} d\eta' \tag{159}$$

$$W_{41} = -[\mathrm{sech}(\eta - \eta_1)]^2 \int_0^\eta [\cosh(\eta' - \eta_1)]^2 \times \times [1 - \tanh(\eta' - \eta_1)] \times \times [\beta_{41} J_2 + W_2(\beta_{42} - \beta_{41}) + W_3(\beta_{43} - \beta_{41})] \frac{1}{\beta_{41}} d\eta' \tag{160}$$

It is easy to see that[17]

$$\eta \to \infty, \quad W_{2,3} \to 0 \tag{161}$$

which coincides with the general result (143). If $a_{1,2} > 0$, then a slow decay of $W_{2,3}$ occurs, in the opposite case $a_{1,2} < 0$ the decay of $W_{2,3}$ is rapid. The analysis show that $W_{2,3}$ reach their maxima at the points $z_{02,03}$, respectively, which are determined by the following expressions:

$$z_{02} = \frac{1}{\beta_{41} J_1} \ln \left[\frac{\beta_{42} W_4(0)}{\beta_{21} W_1(0)} \right] \tag{162}$$

$$z_{03} = \frac{1}{\beta_{41} J_1} \ln \left[\frac{\beta_{43} W_4(0)}{\beta_{31} W_1(0)} \right] \tag{163}$$

The solutions

$$z_{02} > 0, \quad z_{03} > 0$$

exist, if

$$\frac{\beta_{42} W_4(0)}{\beta_{21} W_1(0)} > 1, \quad \frac{\beta_{43} W_4(0)}{\beta_{31} W_1(0)} > 1 \tag{164}$$

The corrections $W_{11,41}$ are finite, small, spatially localized and satisfy the conservation law (152) for any pumping intensity and SA thickness.[17]

Calculating the phases $\gamma_m(z)$ according to the expression[17]

$$\gamma_m - \gamma_m(0) = -\frac{1}{2} \int_0^z \sum_n \delta_{mn} W_n dz' \tag{165}$$

we keep only $W_{10,40}$ neglecting small spatially localized quantities $W_{2,3,11,41}$. Substituting (151) into (165) we find[17]:

$$\gamma_1 = -\frac{\delta_{14}}{2\beta_{41}} \ln\left[\cosh(\eta_1)\exp(\eta)\mathrm{sech}(\eta-\eta_1)\right] \tag{166}$$

$$\gamma_2 = -\frac{1}{2}\ln\{\exp\left(\frac{\delta_{21}+\delta_{24}}{\beta_{41}}\eta\right)\left[\frac{\cosh(\eta-\eta_1)}{\cosh(\eta_1)}\right]^{\mu_1}\} \tag{167}$$

$$\gamma_3 = -\frac{1}{2}\ln\{\exp\left(\frac{\delta_{31}+\delta_{34}}{\beta_{41}}\eta\right)\left[\frac{\cosh(\eta-\eta_1)}{\cosh(\eta_1)}\right]^{\mu_2}\} \tag{168}$$

$$\gamma_4 = -\frac{\delta_{14}}{2\beta_{41}} \ln\left[\mathrm{sech}(\eta_1)\exp(\eta)\cosh(\eta-\eta_1)\right] \tag{169}$$

where

$$\delta_{mn} = \frac{\omega_m^2\omega_n^2 I_0 h_{mn}^2 (\Delta k_{mn\perp})^2}{4\pi\rho c^4 l_m l_n |G_{mn}|^2 (\Delta k_{mn})^2} \times \times\left[(\Delta\omega_{mn})^2 - \Omega_{mn}^2\right] \tag{170}$$

and

$$\mu_1 = \frac{\delta_{21}-\delta_{24}}{\beta_{41}}, \quad \mu_2 = \frac{\delta_{31}-\delta_{34}}{\beta_{41}} \tag{171}$$

It is seen from the expressions (166)-(169) that the phase of the amplified wave E_1 tends to the constant value, while the depletion of the waves $E_{2,3,4}$ is accompanied by the almost periodical cross-phase modulation:

$$\eta \to \infty \quad , \quad \gamma_1 \to -\frac{\delta_{14}}{2\beta_{41}}\ln\left[1+\frac{W_4(0)}{W_1(0)}\right]$$
$$\gamma_{2,3,4} \to -\infty \tag{172}$$

FWM is called polarization-decoupled when some of light waves have perpendicular polarizations.[23] Such waves do not excite the dynamic grating (134) since the corresponding coupling constants vanish, as it is seen from the equations (134), (136) and (141). If each light wave is polarized normal to its incidence plane and therefore propagates as an ordinary one,[20] and one field is perpendicular to the others (for example, $\vec{E}_1 \perp \vec{E}_{2,3,4}$), then we find that the signal wave polarized normal to all other waves propagates through the nonlinear medium without any change. If

$$\vec{E}_1 \perp \vec{E}_{2,3}, \quad \vec{E}_1 \parallel \vec{E}_4 \tag{173}$$

then two independent processes of two-wave mixing occur. The solutions represent two independent pairs of spatial kinks (151)[51] with the different crossing-points (95) and excitation lengths.[17]

In the particular case when the fundamental waves (129) counterpropagate, an analog of BEFWM with a phase conjugation[21] is possible. Consider the situation when the wave E_1 is phase-conjugate of the wave E_4, while the waves $E_{2,3}$ are forward-going and backward-going pumping waves, respectively.[21] The phase-conjugate wave has the time-reversed phase factor with respect to the incident wave.[21] As a result, we obtain from the expression (129):

$$\vec{E}_1 = \vec{e}_1 \left[A_1 \exp i(\vec{k}_4\vec{r} + \omega_1 t) + \text{c.c.}\right] \tag{174}$$

$$\vec{E}_2 = \vec{e}_2 \left[A_2 \exp i(\vec{k}_2\vec{r} - \omega_2 t) + \text{c.c.}\right] \tag{175}$$

$$\vec{E}_3 = \vec{e}_3 \left[A_3 \exp i(\vec{k}_2\vec{r} + \omega_3 t + \Delta\vec{k}_p\vec{r}) + \text{c.c.}\right] \tag{176}$$

$$\vec{E}_4 = \vec{e}_4 \left[A_4 \exp i(\vec{k}_4\vec{r} - \omega_4 t) + \text{c.c.}\right] \tag{177}$$

where $\Delta\vec{k}_p$ is the wave vector mismatch of FWM process.[21]

In the case of the phase conjugation by stimulated scattering the condition of the frequency balance between the harmonics with the same wave vectors is necessary.[21] Choosing the frequency differences

$$\Delta\omega_{31} = \Delta\omega_{42} = \Delta\omega_2 \tag{178}$$

and assuming that the amplitudes of the forward-going and backward-going pumping waves $E_{2,3}$ are large in comparison with the probe wave E_4 and the phase-conjugate wave E_1, and they are kept constant

$$|A_{2,3}| \gg |A_{1,4}|, \quad A_{2,3} = \text{const} \tag{179}$$

we seek the amplitudes of the probe and conjugate waves in the following form:

$$A_{1,4} \sim \exp\left[g_c r \pm i\frac{(\Delta\vec{k}_p\vec{r})}{2}\right] \tag{180}$$

Analysis of the linearized system of the reduced equations (29) for $A_{1,4}$ shows[17] that there exist the root g_{c1} with the negative real part

$$\text{Re}g_{c1} < 0 \tag{181}$$

which corresponds to the amplification of the phase-conjugate wave E_1 propagating in the negative direction. The strong amplification of this wave would occur, if[17]

$$\frac{\varepsilon_a^2 |A_3|^2 \Omega^-}{8\pi B\Gamma^- \sqrt{\varepsilon_\perp \varepsilon_\parallel}} \gg \frac{s_0}{c} \tag{182}$$

The numerical estimations show[17] that this inequality can be easily met for the pumping intensity $\sim 100 MWcm^{-2}$ which is available.[9] The gain coefficient has the form[17]:

$$|\text{Re}g_{c1}| = g_p = \frac{(h^-)^2\Omega^-\mathcal{I}^+}{8\pi Bl(k_z^-)^2\Gamma^-} \tag{183}$$

where

$$\mathcal{I}^+ = \frac{\omega_4^2}{c^2}|A_2|^2 + \frac{\omega_1^2}{c^2}|A_3|^2$$

and

$$\begin{aligned} \vec{k}^- &= \vec{k}_4 - \vec{k}_1 \\ \Delta\omega_2 &= \Omega(\vec{k}^-) = \Omega^- \\ h_{31} &= h_{42} = h^- \\ l &= k_4\left[1 - \frac{(\vec{k}_4\vec{e}_1)}{k_4^2}\right], \quad \Gamma^- = \Gamma(\vec{k}^-) \end{aligned}$$

The phase-matched components of the nonlinear polarization which are normal to the electric field of the fundamental light waves generate their additional components. If the fundamental waves (129) are polarized in the incidence plane, then the transverse components of these waves emerge due to the combination of anisotropy and nonlinearity of SA. These transverse components would be polarized along the unit vectors

$$\vec{e'}_{m\perp} = \frac{[\vec{s}_m \times \vec{e}_m]}{s_m} \tag{184}$$

where $\vec{s}_m$ is a beam vector of the extraordinary wave $\vec{E}_m$, and [20]

$$\vec{s}_m \perp \vec{e}_m$$

Projecting the corresponding part of the wave equation (20) on the direction $\vec{e'}_{m\perp}$ and using the relationships (132) and (133) we obtain:

$$E'_{m\perp} = \frac{\omega_m^2}{s_m c^2 k_m^2}\left(\vec{D}_m^{NL}\cdot[\vec{s}_m \times \vec{e}_m]\right) \tag{185}$$

where $\vec{D}_m^{NL}$ is determined by the expressions (8), (22), (132)-(134), (136) and (137). If the fundamental waves (129) are polarized in the layer plane and perpendicular to the propagation direction, the only component of the nonlinear electric induction which is normal to the field $\vec{E}_m$ is D_{mz}^{NL} since SA is a uniaxial crystal[7,8]:

$$\begin{aligned} D_{mz}^{NL} &= \left[-\varepsilon_a A_m \exp i(\vec{k}_m\vec{r} - \omega_m t)\right] \times \\ &\times \sum_n \frac{a_\perp(\vec{e}_{m\perp}\vec{e}_{n\perp})\Omega_{mn}^2(\Delta\vec{k}_{mn\perp}\vec{e}_{n\perp})}{4\pi B G_{mn}\Delta k_{mnz}}|A_n|^2 + \text{c.c.} \end{aligned} \tag{186}$$

It generates the following field components[17]:

$$E'_{mz} = \frac{k_{m\perp}^2}{(\varepsilon_\perp k_{m\perp}^2 + \varepsilon_\parallel k_{mz}^2)} D_{mz}^{NL} \tag{187}$$

$$E'_{m\perp} = -\frac{k_{mz}(\varepsilon_\parallel k_m^2 + \varepsilon_\perp k_{m\perp}^2)}{\varepsilon_\perp k_{m\perp}(\varepsilon_\perp k_{m\perp}^2 + \varepsilon_\parallel k_{mz}^2)} D_{mz}^{NL} \tag{188}$$

Comparing the relationships (143), (149) and (185)-(188) one may see that all additional components E'_m are finite and spatially localized[17]:

$$z \to \infty, \quad E'_m \to 0 \tag{189}$$

The components of the nonlinear electric induction (58) which are not phase-matched to the fundamental waves (129) give rise to the number of the scattered harmonics with the Stokes and anti-Stokes frequencies:

$$\vec{f}_l^S = \vec{F}_l^S \exp i\psi_l \tag{190}$$

The amplitudes F_l^S in the case of nondegenerate FWM have an order of magnitude of the following expression:

$$F_l^S \sim \frac{\varepsilon_a^2 \left| A_m A_n A_p \right| \Omega_{mn}^2}{4\pi B \left| G_{mn} \right|} \tag{191}$$

where $A_{m,n,p}$ are the amplitudes of the fundamental waves (129). Comparing the expressions (143), (149) and (191) it is seen that all harmonics f_l^S have the finite and spatially localized amplitudes[17]:

$$z \to \infty, \quad \left| F_l^S \right| \to 0 \tag{192}$$

The total number of the scattered harmonics with essentially different frequencies and wave vectors is equal to 24. Indeed, the multiplication of 6 harmonics of the dynamic grating (134) and of 4 fundamental waves (129) yields 48 terms including 12 terms which are phase-matched to the fundamental waves (129).[17] The remaining 36 terms include 12 terms of the type

$$A_m A_p A_n^* \exp i \left[(\vec{k}_m + \vec{k}_p - \vec{k}_n)\vec{r} - (\omega_m + \omega_p - \omega_n)t \right] \tag{193}$$

which are doubly degenerate, and 12 terms of the type[17]

$$A_m^2 A_n^* \exp i \left[2(\vec{k}_m \vec{r} - \omega_m t) - (\vec{k}_n \vec{r} - \omega_n t) \right] \tag{194}$$

5. THE ELECTRODYNAMIC AND HYDRODYNAMIC EXCITATIONS CAUSED BY THE LIGHT-INDUCED LAYER DISPLACEMENT

5.1 The Longitudinal High-Frequency Electric Field in SA

In liquid crystals a specific kind of electric polarization can exist which is connected with the orientational deformations – the so-called flexoelectric polarization.[7,8,52] In the static case the flexoelectric polarization in SA caused by layer normal deformations is negligibly small in comparison with the one in NLC because of the large value of the elastic constant B.[26] However, in the case of the optically excited dynamic grating of the layer normal displacement (134) the flexoelectric polarization in SA can reach the same magnitude as in NLC due to the resonant character of the excitation. The flexoelectric polarization $\vec{P}_f$ in SA has the form[26]:

$$\vec{P}_f = \left[-e_3^f\left(\vec{x}\frac{\partial^2}{\partial z\partial x} + \vec{y}\frac{\partial^2}{\partial z\partial y}\right) - \vec{z}\left(e_1^f\nabla_\perp^2 + e_2^f\frac{\partial^2}{\partial z^2}\right)\right]u \tag{195}$$

where $e_{1,2,3}^f$ are the flexoelectric coupling constants.[26] The polarization (195) causes the electric field $\vec{E}_f$ according to the condition (23)[20]:

$$\operatorname{div}\left(\varepsilon_\perp\vec{E}_{f\perp} + \varepsilon_\parallel E_{fz}\vec{z} + 4\pi\vec{P}_f\right) = 0 \tag{196}$$

Using the Maxwell equations[20] one can show that a magnetic field $\vec{H}_f$ associated with the flexolectric polarization $\vec{P}_f$ (195) is small and can be neglected:

$$H_f \sim \frac{1}{c}\frac{\Delta\omega}{\Delta k}P_f \sim \frac{s_0}{c}\frac{k_m}{\Delta k_{mn}}P_f \ll P_f \tag{197}$$

Therefore the electric field $\vec{E}_f$ is longitudinal[53]:

$$\operatorname{rot}\vec{E}_f = 0 \tag{198}$$

Combining the equations (134), (136), (195), (196) and (198) we obtain[17]:

$$\begin{aligned}\vec{E}_f &= -\frac{i}{B}\sum_{m,n}\Delta\vec{k}_{mn}\frac{h_{mn}\Omega_{mn}^2\left[\left(e_1^f + e_3^f\right)(\Delta k_{mn\perp})^2 + e_2^f(\Delta k_{mnz})^2\right]}{\Delta k_{mnz}G_{mn}\left[\varepsilon_\perp(\Delta k_{mn\perp})^2 + \varepsilon_\parallel(\Delta k_{mnz})^2\right]}\times\\ &\times A_m A_n^* \exp i(\Delta\vec{k}_{mn}\vec{r} - \Delta\omega_{mn}t)\end{aligned} \tag{199}$$

The longitudinal field $\vec{E}_f$ is spatially localized[17]:

$$z \to \infty, \quad |E_f| \to 0 \tag{200}$$

At the interface $z = 0$ the terms E_{fmn} behave as high-frequency spatially periodic surface waves since they cannot penetrate into a linear medium $z < 0$. Actually, according to the boundary conditions[20] the tangential component of the wave vector of each harmonic (199) is continuous at $z = 0$.

$$k_{mn\perp}^L = \Delta k_{mn\perp} \tag{201}$$

The normal component k_{mnz}^L in a linear medium has a purely imaginary value since

$$\left(\frac{\Delta\omega_{mn}}{c}\right)^2 \sim \frac{s_0^2}{c^2}k_m^2 \ll (\Delta k_{mn\perp})^2 \sim k_m^2\sin^2\left(\frac{\Delta\theta}{2}\right) \tag{202}$$

and therefore

$$(k^L_{mnz})^2 = \left(\frac{\Delta\omega_{mn}}{c}\right)^2 - (\Delta k_{mn\perp})^2 < 0 \tag{203}$$

The light-induced electric field $\vec{E}_f$ (199) breaks the inversion symmetry of SA and permits SHG due to the mixing of the high-frequency wave (199) and the fundamental light waves (129) on the cubic susceptibility of an electronic origin $\chi^{(el)}_{ijkl}$. [19] The second harmonic polarization in such a case has the form:

$$\begin{aligned} P_i^{NL}(2\omega_m) \;\sim\;& \chi^{(el)}_{ijkl}(\omega = \omega_m + \omega_n + \Delta\omega_{mn})E_{fj}(\Delta\omega_{mn}) \times \\ & \times E_{mk}(\omega_m)E_{nl}(\omega_n) \end{aligned}$$

The effective quadratic susceptibility $\chi^{(eff)}_{ikl}(\Delta\omega_{mn})$ in our case has a second sound frequency $\Delta\omega_{mn}$, in contrast to the situation with NLC where SHG is caused by a static flexoelectric polarization[54]:

$$\chi^{(eff)}_{ikl} \sim \chi^{(el)}_{ijkl}E_{fj}(\Delta\omega_{mn})$$

Combining the expressions (129) and (199) we obtain:

$$\begin{aligned} P_i^{NL}(2\omega_m) \;\sim\;& -\frac{i}{B}\chi^{(el)}_{ijkl}(2\omega_m)\,|A_n|^2\,A_m^2\,\Delta k_{mnj}e_{mk}e_{nl} \times \\ & \times\frac{h_{mn}\Omega^2_{mn}\left[\left(e_1^f + e_3^f\right)(\Delta k_{mn\perp})^2 + e_2^f(\Delta k_{mnz})^2\right]}{\Delta k_{mnz}G_{mn}\left[\varepsilon_\perp(\Delta k_{mn\perp})^2 + \varepsilon_\parallel(\Delta k_{mnz})^2\right]} \times \\ & \times \exp i(2\vec{k}_m\vec{r} - 2\omega_m t) \end{aligned}$$

This nonlinear polarization would generate a second harmonic.[19]

5.2 A Light-Induced Hydrodynamic Flow in SA

In NLC the orientational motion gives rise to the so-called twist waves, or orientation waves without the hydrodynamic flow of a liquid as a whole.[35–37] In contrast to NLC, in SA any disturbance in the hydrodynamic flow inevitably results in the hydrodynamic flow according to the equations (1) and (6). The normal component v_z can be calculated immediately from (6)[17]:

$$v_z = \sum_{m,n} V_{mn} \exp i(\Delta\vec{k}_{mn}\vec{r} - \Delta\omega_{mn}t) \tag{204}$$

$$V_{mn} = \frac{\Delta\omega_{mn}h_{mn}\Omega^2_{mn}}{4\pi B G_{mn}(\Delta k_{mnz})^2}A_m A_n^* \tag{205}$$

The derivation of the equation of motion (13) shows that the interfering light waves excite the rotational flow having the vorticity[55]

$$\mathrm{rot}\vec{v} \neq 0$$

The hydrodynamic flow (204) is a complicated spatio-temporal pattern[25] which represents a superposition of 6 harmonics with different spatial periods $\sim (\Delta k_{mn})^{-1}$ and temporal periods $\sim (\Delta\omega_{mn})^{-1}$. According to the relationships (127), (131) and (133)

$$k_m \sim k_n \tag{206}$$

For small angles between $\vec{k}_m$ and $\vec{k}_n$

$$\Delta k_{mn} \ll k_m \tag{207}$$

and $\Delta\vec{k}_{mn}$ is approximately normal to the propagation directions of the coupled light waves. Consequently, according to the condition (1) the direction of the hydrodynamic velocity $\vec{v}$ would be approximately parallel to the wave vector $\vec{k}_m$, i.e. it almost coincides with the light wave propagation direction. If additionally the angle between $\vec{k}_{m,n}$ and the Z axis is small, then SA would mainly flow in the direction perpendicular to a layer. In the opposite case, when the light waves propagate under a small angle to a layer plane they give rise to the flow which is almost parallel to a layer plane. Each harmonic in the series (204) can be characterized by two spatial scales. The short scale is determined by the inverse wave vector difference $(\Delta k_{mn})^{-1}$. The large scale is due to the spatial inhomogeneity of the amplitudes A_m, and it is determined by the correlation lengths $(\beta_{mn})^{-1}$. Substituting the relationships (138), (149) and (156) into (205) we obtain[17]:

$$|V_{mn}|^2 = \frac{\beta_{mn} I_0 \Delta\omega_{mn} \Omega_{mn}^2}{4\pi B \Gamma_{mn} (\Delta k_{mnz})^2} M_{mn} \tag{208}$$

where

$$\begin{aligned} M_{mn} &= W_m W_n = W_m(0) W_n(0) \times \\ &\times \exp\left[-\int_0^z \left(\sum_j \beta_{mj} W_j + \sum_i \beta_{ni} W_i\right) dz'\right] \end{aligned} \tag{209}$$

The factor M_{mn} (209) determines the large-scale profile of the hydrodynamic velocity containing the combination of the energetic, temporal and spatial characteristics of the process. Comparing the expressions (209) and (143) we see that all amplitudes V_{mn} are finite and spatially localized.

$$z \to \infty, \quad |V_{mn}| \to 0 \tag{210}$$

Therefore all hydrodynamic excitations are of the convective type.[56]

The analysis[17] shows that the envelopes of the velocity harmonics have the form of a spatial soliton.[51] The hydrodynamic flow is divided into the large-scale strata with the different temporal and short-scale spatial periodicity.[17] If all β_{mn} are essentially different, the points of maximum would be well resolved from one another, and the different strata would be distributed approximately symmetrically with respect to the maximum of the largest component. In the opposite case when all β_{mn} are approximately equal the small components with the rapidly oscillating different phases may be neglected in comparison with the largest component, and the hydrodynamic flow would have the soliton profile of this component. Numerical estimations show that all $|M_{mn}|$ vanish for $\eta \sim (4 \div 5)$. Each amplitude $|V_{mn}|$ reaches its maximal value in the resonant case when the condition (157) is met. The hydrodynamic velocity may reach a maximal value about 10 $cm\ sec^{-1}$. The minimal sample thickness which is sufficient for the excitation of the hydrodynamic spatial soliton in the strong optical field must be of an order of magnitude of the excitation (correlation) length $L_E \sim$ 0.02 cm.[17] The samples of SA of a thickness $\sim (200 \div 500)$ μm have been used to observe SLS and second sound excitation.[9,33,34]

The results obtained are valid for both homeotropically and planary oriented[7,8] SA. The only necessary condition is that light waves should propagate obliquely to smectic layers, or in other words, to the optical axis of SA.

So far we considered SA as a dielectric material. However, it should be noted that in SA with a finite electric conductivity the light-induced hydrodynamic flow can change a character of an electroconvection process.[57] If dc electric field is applied, the electric current in SA consists of the ion fluxes due to migration, diffusion and convection.[57] The light-induced high-frequency hydrodynamic velocity (204) can be greater, than a time-independent migration velocity of ions with a low mobility $\mu \sim 10^{-10}$ m^2/V sec in a dc field $E_{dc} \sim (10^3 \div 10^4)$ V/cm. As a result, the ac component would be predominant, which makes it possible the formation of high-frequency patterns.[25] The comprehensive analysis of this problem is a topic of a perspective work connected with a high-frequency hydrodynamics and electrodynamics of a smectic phase in general.

6. CONCLUSIONS

The new mechanism of the optical nonlinearity determined by the layer notmal displacement $u(\vec{r}, t)$ combines advantages of both orientational and electrostrictive ones:

1. A large magnitude of a cubic nonlinearity in comparison with an ordinary Brillioun nonlinearity due to the smaller magnitude of the corresponding elastic constant;

2. A short time response due to the high viscosity of SA;
3. A weak temperature dependence, at least for temperatures not very close to the phase transition;
4. A resonant form of the frequency dependence;
5. A strong dependence on the polarization and propagation direction of light waves due to the anisotropic dispersion relation of the second sound.

We obtained the following new results.

1. The ordinary and extraordinary beams undergo a self-focusing and a self-trapping in a form of a transverse spatial soliton due to the light-induced layer normal deformations. The self-focusing and self-trapping of the extraordinary beam are possible only when the angle between the propagation direction and the wave vector of the beam caused by an optical anisotropy of SA is sufficiently small. In ordinary crystals such an effect is negligibly small. The nonlinear part of a SA refraction index determined by layer normal deformation is about $10^{-10} esu$ which is one or two orders of magnitude greater than the one for an orientational Kerr effect and electrostiction in isotropic organic liquids. The propagation of a bright surface-guided wave is possible at an interface between a linear medium and SA.[18] The arbitrary polarized light wave propagating in a layer plane undergoes a spatial self-phase modulation, and its polarization plane is changing.
2. The stimulated scattering of two incident arbitrary polarized light waves appeared to be a partly degenerate FWM due to the splitting of each incident wave into the ordinary wave and the extraordinary one. Four coupled light waves create the dynamic grating of the layer normal displacement $u(\vec{r}, t)$ and undergo simultaneously the parametric energy exchange and cross-phase modulation due to the nonlinear scattering on this dynamic grating. When the frequency difference of the coupled waves satisfies the second sound dispersion relation, the strong resonant scattering and second sound wave excitation occur. Two light waves with the lower frequency are amplified, while two light waves with the greater frequency are depleted. The gain coefficient is one or two orders of magnitude greater than the one in isotropic organic liquids. The spectrum of scattered waves consists of 20 harmonics with the Stokes, anti-Stokes and fundamental frequencies, and with the combination wave vectors. The anisotropy and nonlinearity of SA give rise to the additional components of the fundamental light waves.[16]

In the particular case when the incident light waves are polarized strictly in the incidence plane, or normal to it, the two-wave mixing occurs, which is accompanied by the amplification of the wave with the lower frequency, the depletion of the wave with the higher frequency and the cross-phase modulation.[12,14,15] The sufficiently strong incident light wave excites the secondary light wave and the second sound wave. In such a case there exist the threshold of excitation.[13]

3. The nondegenerate FWM in SA results in an excitation of the dynamic grating of the layer normal displacement consisting of 6 components, and in an energy exchange among the coupled light waves due to the new mechanism of the optical nonlinearity caused by the layer displacement. The light wave with the lowest frequency is amplified up to a saturation level. The light wave with the highest frequency decreases monotonically, and it is finally totally depleted. The two light waves with intermediate frequencies form the spatially localized structures. If the input pumping-signal intensity ratio is high enough, a limited spatial interval exist where three light waves with lower frequencies are amplified. In the special case of the counterpropagating waves and frequency balance which is typical for a phase-conjugation process an analog of BEFWM occurs with the amplification of a phase-conjugate wave. The combination of anisotropy and nonlinearity of SA results in the generation of the additional components of the fundamental light waves. The scattering of the fundamental light waves on the dynamic grating generates the spectrum of 24 Brillouin-like small harmonics with the Stokes and anti-Stokes frequencies and combination wave vectors.[17] The numerical estimations for the typical values of the material parameters and the pumping intensity yield the values of the gain coefficient and excitation length which are in accord with the experimental data.[9]

4. As a result of the flexoelectric effect[7,8,26,52] the light-induced dynamic grating of layer displacement generates a longitudinal high-frequency electric field. This electric field does not penetrate into a linear medium and behaves as a surface wave at the boundary between linear medium and SA.[15–17] The light-induced electric field breaks the inversion symmetry of SA and permits SHG.

5. A light-induced layer displacement results in the excitation of a hydrodynamic flow which represents a complicated spatio-temporal pattern with two different spatial scales. The short scale is determined by the wave vectors of the dynamic grating harmonics. The large scale is characterized

by the same excitation (correlation) lengths as the process of the light wave amplification (depletion). All harmonics of the hydrodynamic velocity are spatially localized. The hydrodynamic velocity may reach a value of 10 cm sec^{-1}. The hydrodynamic flow can be stratified, or can possess a soliton-like spatial profile.[17]

ACKNOWLEDGEMENTS

One of the authors (B. L.) is very grateful to the "Bat Sheva de Rotshild Foundation for the Advancement of Science in Israel" for the financial support of this work.

REFERENCES

1. I. C. Khoo and S. T. Wu, Optics and Nonlinear Optics of Liquid Crystals (World Scientific, Singapore, 1993), Chap. 1, pp. 51-60, 72-90, chap. 3, pp. 269-350.
2. S. M. Arakelyan, G. A. Lyakhov, Yu. S. Chilingaryan, Sov. Phys. Uspekhi, 23, 245, (1980).
3. S. M. Arakelyan, Yu. S. Chilingaryan, Nonlinear Optics of Liquid Crystals (Nauka, Moscow, 1984) (in Russian), Chap. 2, pp. 55-56, Chap. 3, pp. 112-153, Conclusion, pp. 323-325.
4. B. Ya. Zel'dovich and N. V. Tabiryan, Sov. Phys. Uspekhi, 28, 1059, (1985).
5. I. C. Khoo, in Progress in Optics, edited by E. Wolf (North Holland, Amsterdam, 1988), vol. 26, Chap. 1, pp. 107, 108, Chap. 2, pp. 115, 127, chap. 3, pp. 133-144, 149-152.
6. Ansgar Scmid, Semyon Papernov, Zheng-Wu Li, Mark Guardalben and Stephen D. Jacobs, Mol. Cryst. Liq. Cryst., 207, 33, (1991).
7. S. Chandrasekhar, Liquid Crystals (Second Edition) (Cambridge University Press, New York, 1992), Chap. 5, pp. 300, 301, 310-325.
8. P. G. de Gennes and J.Prost, The Physics of Liquid Crystals (Second Edition) (Clarendon, Oxford, 1993), Chap. 1, pp. 10-12, Chap. 3, pp. 102-104, chap. 7, pp. 337-339, chap. 8, pp. 421-423.
9. Iam-Choon Khoo, Robert R.Michael, Jr. and Pei-Yang Yan, IEEE J. of Quant. Electr., QE-23, 1344, (1987).
10. I. C. Khoo, R. G. Lindquist, R. R. Michael, R. J. Mansfield, and P. LoPresti, J. Appl. Phys. (USA), 69, 3853 (1991).
11. V. A. Balandin, E. V. Gurovich, A. S. Kashitsin, and S. V. Pasechnik, Liquid Crystals, 9, 551 (1991).

12. B. I. Lembrikov, Sov. Phys. Technical Physics, 25, 1145 (1980).
13. B. I. Lembrikov, Sov. Phys. Solid State, 23, 715 (1981).
14. B. I. Lembrikov, Sov. Phys. Technical Physics, 27, 923 (1982).
15. G. F. Kventsel and B. I. Lembrikov, Liquid Crystals, 16, 159 (1994).
16. G. F. Kventsel and B. I. Lembrikov, Liquid Crystals, 19, 21 (1995).
17. G. F. Kventsel and B. I. Lembrikov, Mol. Cryst. Liq. Cryst., 262, 591 (1995).
18. G. F. Kventsel and B. I. Lembrikov, Mol. Cryst. Liq. Cryst., 262, 629 (1995).
19. Y. R. Shen, The Principles of Nonlinear Optics (John Wiley, New York, 1984), Chap. 3, pp. 42-52, Chap. 11, pp. 187-201.
20. L. D. Landau and E. M. Lifshitz, Electrodynamics of Continuous Media (Second Edition) (Pergamon, Oxford, 1984), Chap. 2, pp. 35, 54, 55, Chap. 9, p. 257, Chap. 10, pp. 293, 294, Chap. 11, pp. 333-340, Chap. 12, p. 358.
21. Robert W. Boyd and Gylbert Grynberg, in Contemporary Nonlinear Optics, edited by Govind P. Agarwal and Robert Boyd (Academic Press, New York, 1992), Chap. 3, pp. 86-106.
22. A. M. Scott and K. D. Ridley, IEEE J. of Quant. Electr., 25, 438 (1989).
23. W. A. Schroeder, M. J. Damzen and M. H. R. Hutchinson, IEEE J. of Quant. Electr., 25, 460 (1989).
24. V. F. Efimkov, I. G. Zubarev, S. A. Pastukhov, and V. B. Sobolev, Sov. J. Quantum Electronics, 22, 62 (1992).
25. M. C. Gross, P.C. Hohenberg, Rev. Mod. Phys., 65, 851 (1992), Chap. 1, pp. 851-857, Chap. 7, pp. 940-941.
26. P. G. de Gennes, J. de Physique, Colloque C4, 30, C4-65 (1969).
27. M. J. Stephen and J. P. Straley, Rev. Mod. Phys., 46, 617 (1974).
28. P. C. Martin, O. Parodi and P. S. Pershan, Phys. Rev. A, 6, 2401 (1972).
29. L. D. Landau and E. M. Lifshitz, Theory of Elasticity (Third Edition) (Pergamon, Oxford, 1986), Chap. 6, pp. 179 - 184.
30. E. I. Kats, V. V. Lebedev, Dynamics of Liquid Crystals (Nauka, Moscow, 1988) (in Russian), Chap. 2, pp. 126-149.
31. G. A. Korn, T. M. Korn, Mathematical Handbook (Mc Graw-Hill, New York, 1968), Chap. 5.5-6, p. 161, Chap. 9.1-3, p. 246, Chap. 9.2-4, p. 250.
32. York Liao, Noel A. Clark and P. S. Pershan, Phys. Rev. Lett., 30, 639 (1973).
33. L. Ricard and J. Prost, J. de Physique, Colloque C3, 40, C3-83 (1979).
34. L. Ricard and J. Prost, J. de Physique, 42, 861 (1981).
35. J. L. Ericsen, The Quaterly Journal of Mechanics and Applied Mathematics, 21, 463 (1968).
36. A. Saupe, Mol. Cryst. Liq. Cryst., 7, 59 (1969).

37. J. L. Ericsen, Mol. Cryst. Liq. Cryst., 7, 153 (1969).

38. O. Svelto, in Progress in Optics, edited by E.Wolf (North Holland, Amsterdam, 1974), vol. 12, Chap. 1, pp. 3, 4, 10, Chap. 2, pp. 14, 23, 24, Chap. 3, pp. 25, 26.

39. R. Y. Chiao, E. Garmire and C. H. Townes, Phys. Rev. Lett., 13, 479 (1964).

40. V. E. Zakharov, A. B. Shabat, Sov. Phys. JETP, 34, 62 (1972).

41. Govind P. Agarwal, in Contemporary Nonlinear Optics, edited by Govind P. Agarwal and Robert Boyd (Academic Press, New York, 1992), Chap. 2, pp. 76-78.

42. A. P. Sukhorukov, The Nonlinear Interactions of Waves in Optics and Radiophysics (in Russian) (Nauka, Moscow, 1988), Chap. 1, pp. 15-16.

43. V. G. Dmitriev, G. G. Gurzadyan and D. N. Nikogosyan, Handbook of Nonlinear Optical Crystals (Springer Verlag, Berlin, 1991), Chap. 3, pp. 74-94.

44. Edward Collett, Polarized Light (Marcel Dekker, New York, 1993), Chap. 4, pp. 34-38.

45. Yijing Chen and Allan W. Snyder, Optics Letters, 14, 87 (1989).

46. Yijing Chen, J. Opt. Soc. Am. B, 6, 1986 (1989).

47. B. Kryzhanovsky and A. Karapetyan and B. Glushko, Phys. Rev. A, 44, 6036 (1991).

48. B. Kryzhanovsky and Boris Glushko, Phys. Rev. A, 45, 4979 (1992).

49. V. S. Starunov and I. L. Fabelinskii, Sov. Physics Uspekhi, 12, 463 (1970).

50. Amnon Yariv, Quantum Electronics (Second Edition), (John Wiley, New York, 1975), Chap. 19, p. 498.

51. R. K. Dodd, J. C. Eilbeck, J. D. Gibbon, H. C.Morris, Solitons and Nonlinear Wave Equations (Academic Press, London, 1984), Chap. 1, pp. 31-33.

52. Jacques Prost and P. S. Pershan, J. Appl. Phys. (USA), 47, 2298 (1976).

53. L. D. Landau and E. M. Lifshitz, The Classical Theory of Fields (Fourth Edition) (Pergamon, Oxford, 1989), Chap. 6, p. 125.

54. S. M. Arakelyan, G. L. Grigoryan, A. S. Karayan, S. Ts. Nersisyan, and Yu. S. Chilingaryan, Sov. Phys. Solid State, 26, 806 (1984).

55. L. D. Landau and E. M. Lifshitz, Fluid Mechanics (Second Edition) (Pergamon, Oxford, 1987), Chap. 1, pp. 13, 14, 17.

56. E. M. Lifshitz and L. P. Pitaevskii, Physical Kinetics (Pergamon, Oxford, 1981), Chap. 6, pp. 268-276.

57. Stephen W. Morris, John R. de Bruyn, A. D. May, Phys. Rev. A, 44, 8146 (1991).